

Accepted Manuscript

Identification of 3-substituted-6-(1-(1*H*-[1,2,3]triazolo[4,5-*b*]pyrazin-1-yl)ethyl)quinoline derivatives as highly potent and selective mesenchymal-epithelial transition factor (c-Met) inhibitors via metabolite profiling-based structural optimization

Fei Zhao, Le-Duo Zhang, Yu Hao, Na Chen, Rui Bai, Yu-Ji Wang, Chun-Chun Zhang, Gong-Sheng Li, Li-Jun Hao, Chen Shi, Jing Zhang, Yu Mao, Yi Fan, Guang-Xin Xia, Jian-Xin Yu, Yan-Jun Liu

PII: S0223-5234(17)30253-2

DOI: [10.1016/j.ejmech.2017.03.085](https://doi.org/10.1016/j.ejmech.2017.03.085)

Reference: EJMECH 9345

To appear in: *European Journal of Medicinal Chemistry*

Received Date: 21 January 2017

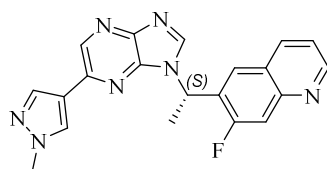
Revised Date: 28 March 2017

Accepted Date: 31 March 2017

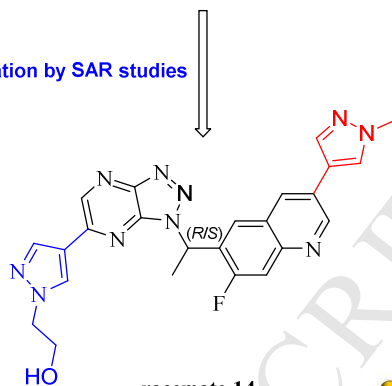
Please cite this article as: F. Zhao, L.-D. Zhang, Y. Hao, N. Chen, R. Bai, Y.-J. Wang, C.-C. Zhang, G.-S. Li, L.-J. Hao, C. Shi, J. Zhang, Y. Mao, Y. Fan, G.-X. Xia, J.-X. Yu, Y.-J. Liu, Identification of 3-substituted-6-(1-(1*H*-[1,2,3]triazolo[4,5-*b*]pyrazin-1-yl)ethyl)quinoline derivatives as highly potent and selective mesenchymal-epithelial transition factor (c-Met) inhibitors via metabolite profiling-based structural optimization, *European Journal of Medicinal Chemistry* (2017), doi: 10.1016/j.ejmech.2017.03.085.

This is a PDF file of an unedited manuscript that has been accepted for publication. As a service to our customers we are providing this early version of the manuscript. The manuscript will undergo copyediting, typesetting, and review of the resulting proof before it is published in its final form. Please note that during the production process errors may be discovered which could affect the content, and all legal disclaimers that apply to the journal pertain.



**compound 1**IC₅₀ = 1.45 nM (enzyme)IC₅₀ = 24.7 nM (H1993)IC₅₀ = 11.8 nM (SNU-5)Metabolite profiling-based
structural optimization

Filtration by SAR studies

**racemate 14**IC₅₀ = 0.6 nM (enzyme)IC₅₀ = 1.1 nM (H1993)IC₅₀ = 2.0 nM (SNU-5)T_{1/2} = 3.7 h *F* = 12.1%**Xenograft models**

H1993 TGI (10mg/kg): 90.8%

SNU-5 PTR (3mg/kg): 87.9%

ACCEPTED MANUSCRIPT

Identification of
3-substituted-6-(1-(1*H*-[1,2,3]triazolo[4,5-*b*]pyrazin-1-yl)ethyl)quinoline
derivatives as highly potent and selective mesenchymal-epithelial transition
factor (c-Met) inhibitors via metabolite profiling-based structural optimization

Fei Zhao, Le-Duo Zhang, Yu Hao, Na Chen, Rui Bai, Yu-Ji Wang, Chun-Chun Zhang,
Gong-Sheng Li, Li-Jun Hao, Chen Shi, Jing Zhang, Yu Mao, Yi Fan, Guang-Xin Xia,
Jian-Xin Yu*, Yan-Jun Liu*

Central Research Institute, Shanghai Pharmaceuticals Holding Co., Ltd., Building 5, No. 898
Halei Road, Shanghai 201203, P. R. China

ABSTRACT:

c-Met/HGF signaling pathway plays an important role in cancer progression, and it was considered to be related to poor prognosis and drug resistance. Based on metabolite profiling of (S)-7-fluoro-6-(1-(6-(1-methyl-1*H*-pyrazol-4-yl)-1*H*-imidazo[4,5-*b*]pyrazin-1-yl)ethyl)quinoline (**1**), a series of 2-substituted or 3-substituted-6-(1-(1*H*-[1,2,3]triazolo[4,5-*b*]pyrazin-1-yl)ethyl)quinoline derivatives was rationally designed and evaluated. Most of the 3-substituted derivatives not only exhibited potent activities in both enzymatic and cellular assays, but also were stable in liver microsomes among different species (human, rat and monkey). SAR investigation revealed that introducing of

* Corresponding authors. Tel.: +86 21 61871700; Fax: +86 21 50128885.
E-mail addresses: yujx@sphchina.com (J.-X. Yu), liuyj@sphchina.com (Y.-J. Liu).

N-methyl-1*H*-pyrazol-4-yl group at the 3-position of quinoline moiety is beneficial to improve the inhibitory potency, especially in the cellular assays. The influence of fluorine atom at 7-position or 5, 7-position of quinoline moiety and substituents at the 6-position of triazolo[4,5-*b*]pyrazine core on overall activity is not very significant. Racemate **14**, an extremely potent and exquisitely selective c-Met inhibitor, demonstrated favorable pharmacokinetic properties in rats, no significant AO metabolism, and effective tumor growth inhibition in c-Met overexpressed NSCLC (H1993 cell line) and gastric cancer (SNU-5 cell line) xenograft models. Docking analysis indicated that besides the typical interactions of most selective c-Met inhibitors, the intramolecular halogen bond and additional hydrogen bond interactions with kinase are beneficial to the binding. These results may provide deep insight into potential structural modifications for developing potent c-Met inhibitors.

Keywords: c-Met; 3-Substituted quinolines; Triazolopyrazine; Metabolism; SAR; Docking study

1. Introduction

The tyrosine kinase mesenchymal-epithelial transition factor (c-Met), encoded by MET proto-oncogene, belongs to a structurally distinct subfamily of receptor tyrosine kinase (RTK) and its endogenous ligand is hepatocyte growth factor (HGF, also known as scatter factor (SF)) [1]. c-Met/HGF signaling pathway plays an important role in a diverse array of biological activities which are essential in the development of mammalian cells, such as cell proliferation, survival, motility and wound healing, etc. However, this pathway is also implicated in tumor angiogenesis, invasion and metastasis, etc [2-5]. Abnormal c-Met/HGF signaling has been found in a number of major human malignancies and was related to poor prognosis and high tumors grade [6-10].

Furthermore, aberrant c-Met signaling was demonstrated to be associated with the resistance of tumor cells during chemotherapy, radiotherapy and other RTK based target therapy such as epidermal growth factor receptor (EGFR) inhibitors [11, 12].

Given its critical role in tumor cell biology, c-Met is emerging as an attractive oncology target. Until now, two generations of ATP-competitive small molecule c-Met inhibitors with different selectivity profiles have been developed. Among them, Crizotinib (PF-02341066) [13] and Cabozantinib (XL184) [14] have been approved for the treatment of non-small cell lung carcinoma (NSCLC) and medullary thyroid cancer (MTC) in 2011 and 2012, respectively. However, both of them acted on other kinases besides c-Met, so far none of selective c-Met inhibitor has been approved. During the past decade, a great deal of effort has been made to the discovery of potent and exquisitely selective c-Met inhibitors [15-19]. These have enjoyed some successes. Dozens of drug candidates progressed to human clinical studies and several of them achieved clinical benefits in a variety of cancers, such as INCB28060 [20], Volitinib [21] and AMG 337 [22], etc (**Fig. 1**).

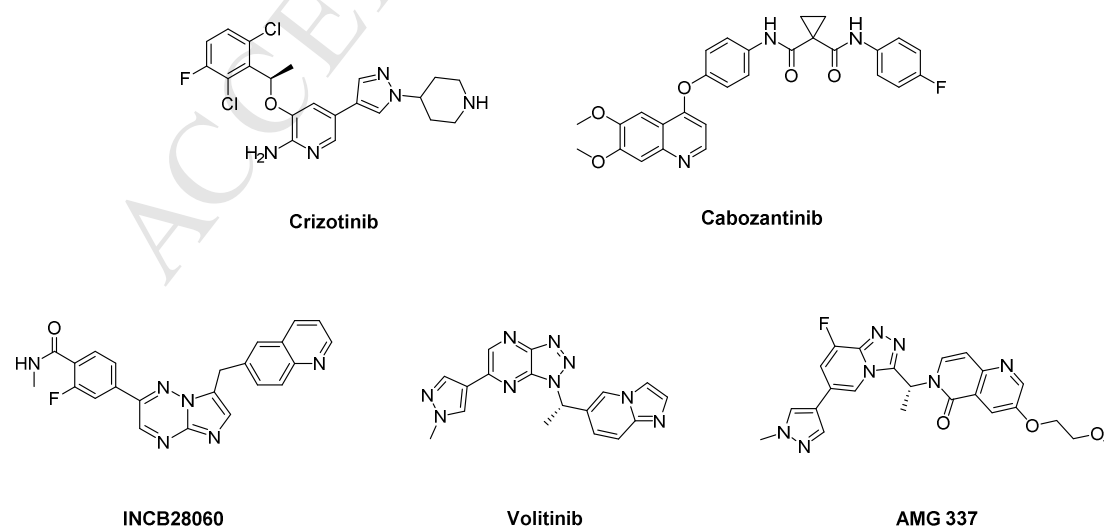


Fig. 1. Reference compounds.

In our previous studies, a series of imidazo[4,5-*b*]pyrazine derivatives as potent and selective inhibitor of c-Met kinase was discovered. Medicinal chemistry lead optimization produced (*S*)-7-fluoro-6-(1-(6-(1-methyl-1*H*-pyrazol-4-yl)-1*H*-imidazo[4,5-*b*]pyrazin-1-yl)ethyl)quinoline (compound **1**) as a promising c-Met inhibitor [23]. Unfortunately, a further evaluation of this compound incubated with monkey liver microsomes (MLM) demonstrated it was metabolized rapidly via both NADPH-dependent and NADPH-independent enzymes, which posed a concern on the druggability of this scaffold. A metabolite profiling of compound **1** was then conducted to investigate the major metabolites. As shown in **Fig. 2**, there are two main products generated in MLM (incubated with or without NADPH): imidazole-oxide **M1** and quinoline *N*-oxide **M2**. In order to improve ADME properties of this scaffold, the strategy we employed is to block metabolism by means of modifying the metabolically labile sites. Our earlier SAR investigation revealed that the introduction of a methyl group or hydroxyl group at the 2-position of imidazole ring resulted in the loss of c-Met inhibitory potency [23]. Considering the important π - π stacking interaction between this fused ring and electron-rich Tyr-1230 of the kinase, a much more electron-deficient and more metabolically stable [1,2,3]triazolo[4,5-*b*]pyrazine ring, by means of bioisosteric replacement of imidazo[4,5-*b*]pyrazine, was selected in our follow-up study. On the other hand, although great efforts have been made to replace the conserved quinoline moiety of the second generation c-Met inhibitors due to the reported aldehyde oxidase (AO, a NADPH-independent enzyme) mediated toxicity of SGX523 which was discontinued in clinical development [21, 24], our experimental data indicated that the major AO-mediated metabolite of compound **1** is imidazo-oxidized product **M1** and none of any quinoline-oxides was detected.

Additionally, the nitrogen atom of quinoline hinge motif was confirmed by several literatures to participate in a hydrogen bond with the backbone NH of Met-1160, which is crucial for selective binding to c-Met kinase [15, 21, 25, 26]. Taken together, it is reasonable to maintain this ubiquitous quinoline group in our next study. Here, with the hope of reducing the formation of *N*-oxide by increasing steric hindrance of biological oxidation, large substituents were attached to the 2-position or 3-position of quinoline moiety.

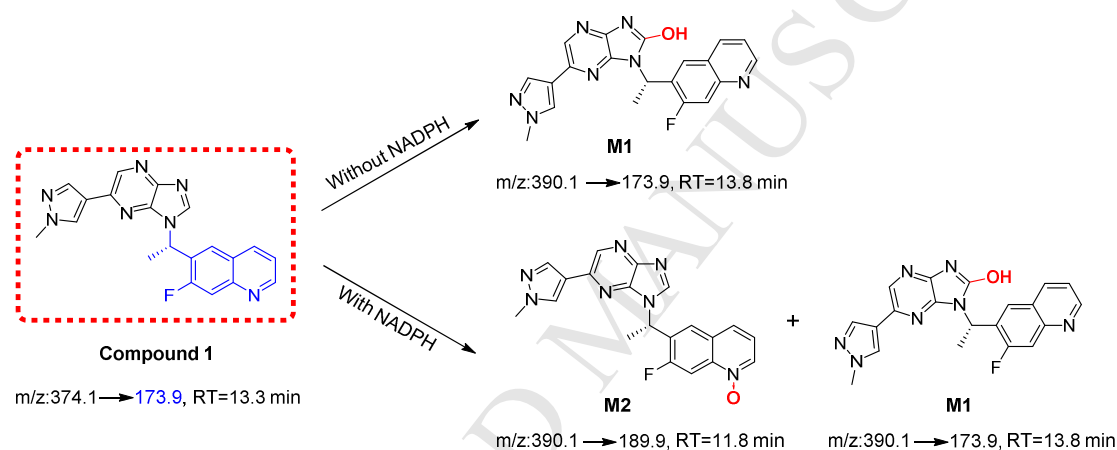


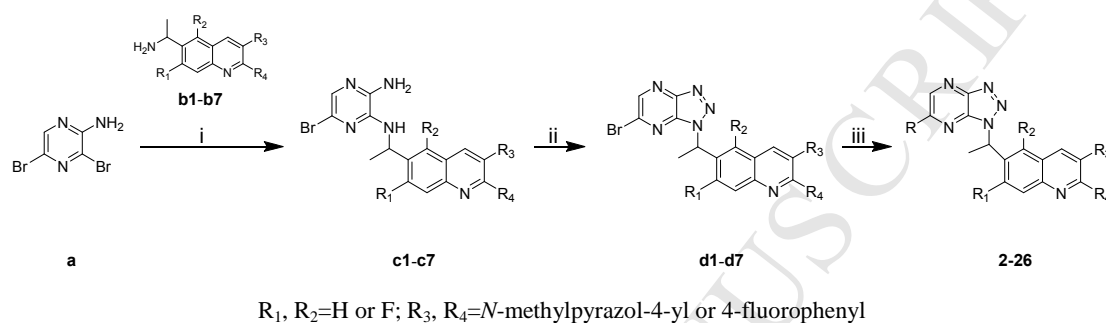
Fig. 2. Major metabolites of compound **1** in monkey liver microsomes incubated with or without NADPH.

2. Results and discussion

2.1. Chemistry

Outlined in **Scheme 1** is the synthesis of the title compounds **2-26**. A nucleophilic substitution reaction of commercially available 2-amino-3,5-dibromopyrazine (**a**) with corresponding substituted quinolin-6-ylethan-1-amine (**b1-b7**) in the presence of *N,N*-diisopropyl ethylamine (DIPEA) afforded corresponding 6-bromo-*N*²-(1-(quinolin-6-yl)ethyl)pyrazine-2,3-diamine

intermediates (**c1-c7**). Subsequently **c1-c7** were reacted with isopentyl nitrite to give 6-(1-(6-bromo-1*H*-[1,2,3]triazolo[4,5-*b*]pyrazin-1-yl)ethyl)quinoline intermediates (**d1-d7**), followed by Suzuki coupling with corresponding boric acid or boric acid ester to produce title compounds **2-26**.



Scheme 1. Synthetic procedures of title compounds **2-26**. Reagents and conditions: (i) DIPEA, NMP, 180°C, overnight; (ii) isopentyl nitrite, DMF, 80°C, 2h; (iii) corresponding boric acid or boric acid ester, Pd(dppf)₂Cl₂·DCM complex, K₂CO₃, 1,4-dioxane/H₂O, 110°C, 3h or overnight.

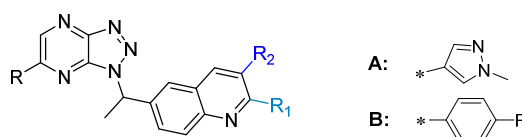
2.2 Biological evaluation

Firstly, seven compounds (**2-8**) were synthesized and enzymatic assay was used as the primary screening. As **Table 1** shows, 3-substituted derivatives (**5-8**) displayed very potent inhibitory activities toward c-Met. Quite unexpectedly, the introduction of a group at the 2-position of quinoline moiety resulted in a dramatic decrease in potency, as illustrated with derivatives **2-4**. 3-Substituted compounds were further evaluated in cellular assays, including c-Met overexpressed human NSCLC H1993 cell line and gastric cancer SNU-5 cell line. Much to our delight, compared with compound **1** all these compounds exhibited a significant increase of potency in both cellular

assays with IC₅₀ values at or even below a single-digit nanomolar level, which is equivalent to the positive control INCB28060.

Table 1

SAR of 2-substituted and 3-substituted quinoline derivatives **2-8**.



Compd.	R ₁	R ₂	R	IC ₅₀ ^a (nM)		
				Enzyme	H1993	SNU-5
1 [23]				1.5	24.7	11.8
2	-A	-H		>100	- ^b	- ^b
3	-A	-H		66.7	- ^b	- ^b
4	-A	-H		>100	- ^b	- ^b
5	-H	-A		0.5	- ^b	0.5
6	-H	-B		1.3	1.2	2.2
7	-H	-B		3.5	4.2	3.7
8	-H	-B		2.6	8.7	7.0
INCB28060				0.4	2.3	2.7

^aIC₅₀ are based on triple runs of experiments.

^bThe – indicates not tested.

Besides the inhibitory activities *in vitro*, what we concerned most is the metabolic stability of this series of compounds, especially in MLM. As shown in **Table 2**, all compounds were stable in liver microsomes among different species (human, rat and monkey). More significantly, the metabolic stability in MLM was improved remarkably, which fully supported our previous molecular design. 3-Substituted-6-(1-(1*H*-[1,2,3]triazolo[4,5-*b*]pyrazin-1-yl)ethyl)quinoline scaffold was therefore identified as core structure and the potential of this series was further explored.

Table 2

Metabolic stability data of compounds in liver microsomes among different species.

Compd.	CL _{int} (μl/min/mg protein) ^a / Parent drug recovery (%) ^b		
	HLM ^c	RLM ^d	MLM ^e
1	8 / 92	49 / 79	- ^f / 1
5	12 / 123	22 / 115	42 / 79
6	16 / 105	28 / 97	112 / 109
7	15 / 104	57 / 97	119 / 93
8	14 / 105	56 / 91	65 / 97

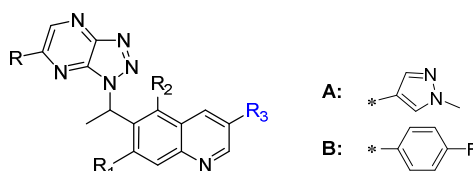
^aCL_{int} was determined with the cofactor NADPH; ^brecovery was determined without the cofactor NADPH; ^chuman liver microsomes; ^drat liver microsomes; ^emonkey liver microsomes; ^fThe-indicates the data was not obtained because of rapid metabolism of compound.

Previous detailed SAR study on imidazo[4,5-*b*]pyrazine series pointed out the introduction of

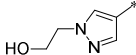
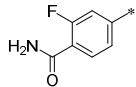
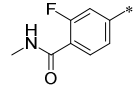
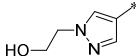
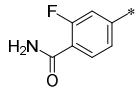
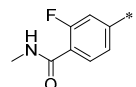
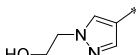
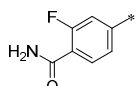
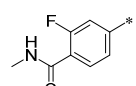
fluorine atom at 7-position or 5, 7-position of quinoline moiety could improve inhibitory activities to some degree in both enzymatic and cellular assays [23]. Therefore, the contribution of fluorine atom to overall activity was also evaluated in the following SAR exploration of 3-substituted-6-(1-(1*H*-[1,2,3]triazolo[4,5-*b*]pyrazin-1-yl)ethyl)quinoline derivatives. As listed in **Table 3**, all compounds showed high potency toward c-Met, especially for compounds substituted with *N*-methylpyrazol-4-yl group at the 3-position of quinoline moiety (**9-22**, $IC_{50} \leq 1$ nM). Most compounds displayed much more potent inhibitory activities than INCB28060 in H1993 cell line, except for compounds **17** and **21** (not tested). Analogues **23-26** with a 4-fluorophenyl group at the 3-position exhibited relatively weak inhibitory activities in both enzymatic and H1993 cell line assays. With the exception of compounds **24** and **26**, all the synthesized compounds displayed much more potent activities than INCB28060 in SNU-5 cell line assay. The kinds of substituents at 6-position of triazolo[4,5-*b*]pyrazine core could influence the inhibitory potency, albeit not very significant. Different from SAR of imidazo[4,5-*b*]pyrazine series, it seems the introduction of fluorine atom on the quinoline moiety has little effect on the overall activity of this series.

Table 3

SAR about the 3-substituted quinoline derivatives.



Compd.	R ₁	R ₂	R ₃	R	IC ₅₀ ^a (nM)		
					Enzyme	H1993	SNU-5

9	-H	-H	-A		0.5	0.2	1.8
10	-H	-H	-A		0.7	0.9	0.7
11	-H	-H	-A		0.5	0.5	0.6
12	-H	-H	-A		0.3	0.9	1.2
13	-F	-H	-A		0.7	0.9	1.7
14	-F	-H	-A		0.6	1.1	2.0
15	-F	-H	-A		0.6	0.9	0.6
16	-F	-H	-A		1.0	1.1	0.6
17	-F	-H	-A		0.7	3.2	2.5
18	-F	-F	-A		0.4	0.8	1.3
19	-F	-F	-A		0.4	0.8	1.3
20	-F	-F	-A		0.3	0.4	0.4
21	-F	-F	-A		0.9	- ^b	0.9
22	-F	-F	-A		0.5	0.2	1.2
23	-F	-H	-B		1.5	4.1	2.0
24	-F	-H	-B		1.7	3.6	6.8
25	-F	-F	-B		3.8	2.6	2.2
26	-F	-F	-B		4.3	3.5	7.2
INCB28060					0.4	2.3	2.7

^aIC₅₀ are based on triple runs of experiments.

^bThe - indicates not tested.

Given decreased potencies of derivatives with 4-fluorophenyl group, this type was discontinued in our next study. Compounds **9-22** were subsequently evaluated for metabolic stability in liver microsomes and inhibition effect on 5CYPs in HLM (1A2, 2C9, 2C19, 2D6 and 3A4), respectively (**Table 4**). Except for compounds **21** and **22**, the vast majority of these compounds were stable in the tested liver microsomes with acceptable clearance ($CL_{int} < 100 \mu\text{l}/\text{min}/\text{mg}$ protein). After incubation for 30 min in liver microsomes among different species (without NADPH), most compounds demonstrated satisfactory recovery with the exception of compounds **13**, **16** and **18** (recovery < 80% in MLM). Many compounds displayed a certain degree of direct inhibition (DI) or time-dependent inhibition (TDI) effect on 5CYPs in HLM, but compounds **14**, **15** and **16** were exceptions.

Table 4

Leadlikeness assessment *in vitro* of compounds **9-22**.

Compd.	CL _{int} (μl/min/mg protein) / Parent drug recovery (%)			DI ^a	TDI ^b
	HLM	MLM	RLM		
9	0 / 105	16 / 108	6 / 104	2C9,2C19	NI ^c
10	3 / 120	30 / 98	10 / 128	NI ^c	3A4,2D6,2C9,1A2
11	1 / 115	16 / 97	5 / 114	3A4	NI ^c
12	22 / 104	78 / 90	61 / 94	3A4	NI ^c
13	5 / 101	11 / 65	34 / 103	NI ^c	3A4
14	5 / 95	50 / 107	5 / 101	NI ^c	NI ^c
15	2 / 120	6 / 103	1 / 115	NI ^c	NI ^c
16	5 / 116	24 / 69	12 / 111	NI ^c	NI ^c
17	4 / 113	49 / 103	55 / 106	3A4,2C9,2C19	NI ^c

18	17 / 91	86 / 75	22 / 94	2C9,2C19	3A4
19	8 / 98	43 / 102	20 / 97	2C9, 2C19	NI ^c
20	11 / 97	50 / 99	12 / 94	NI ^c	3A4
21	5 / 92	187 / 95	48 / 95	2C9, 2C19	NI ^c
22	9 / 101	106 / 99	26 / 98	3A4,2D6,2C9,2C19	NI ^c

^adirect inhibition on 5CYPs in HLM, referred to reversible inhibition, is assessed without a preincubation step.

^btime-dependent inhibition on 5CYPs in HLM, referred to irreversible inhibition, is assessed with a preincubation

step. ^cThe NI indicates inhibition ratio < 50%.

Compounds **14** and **15** were selected for further evaluation of pharmacokinetic properties *in vivo* (**Table 5**). These two compounds displayed similar pharmacokinetic profiles including moderate clearance, equivalent apparent volume of distribution, and acceptable half-life. The bioavailability of compound **14** was a little higher than **15**.

Table 5

In vivo pharmacokinetic profiles^a of compounds **14** and **15**.

Compd.	CL _{plasma} ^b (L/h/kg)	V _{ss} ^b (L/kg)	T _{1/2} ^b (h)	C _{max} ^c (ng/ml)	AUC _{0-24h} ^c (ng·h/ml)	F ^c (%)
14	0.58	2.1	3.7	134.6	1254	12.1
15	0.56	2.0	3.2	98.9	879	8.2

^aExperiments were carried out with male Sprague-Dawley rats (n=2-3). Dose: iv, 1mg/kg; po, 6 mg/kg.

^bParameters obtained after iv dosing. ^cParameters obtained after po dosing.

A panel of 18 human tyrosine kinases was used to investigate the selectivity profile of compound **14**, including highly homologous kinase AXL (tyrosine-protein kinase receptor UFO) and c-Met family member RON (macrophage-stimulating protein receptor). As **Table 6** shows,

this compound is highly selective for c-Met, showing an IC_{50} of >700 nM against other tested tyrosine kinases. Furthermore, in the light of the reported AO-mediated toxicity of SGX523, a metabolite profiling of compound **14** in monkey cytosol was also investigated. After being coincubated with and without the AO inhibitor (Menadione) at $37^{\circ}C$ for 30 min, the relative amounts of **14** are 99.6% and 99.4%, respectively. It revealed that the overall majority is parent and the amount of AO-mediated metabolite is very small. Therefore, we think the AO metabolism will not be significant for this compound and will not lead to a safety concern in humans.

Table 6Kinase-selectivity profile^a of compound **14**.

kinase	IC_{50} (nM)	kinase	IC_{50} (nM)
AxI	1075	EGFR	>30000
RON	731	EGFR[T790]	>30000
ALK	>30000	ErbB4	>30000
Fit-1	>30000	c-Src	17056
VEGFR2	18364	ABL	>30000
c-Kit	5396	EPH-A2	>30000
PDGFRa	2357	EPH-B2	>30000

PDGFRb	>30000	IGF1R	>30000
RET	>30000	FGFR1	>30000

^aCompound **14** against 18 kinases *in vitro* were assayed with ATP concentration at Km.

Our previous study on imidazo[4,5-*b*]pyrazine series indicated that compounds with an (*S*)-configuration displayed more excellent activities than their corresponding (*R*)-configured compounds in both enzymatic and cellular assays [23]. Accordingly, the two enantiomers of compound **14** were obtained by chiral chromatography and further evaluated. Unexpectedly, these two enantiomerically pure compounds displayed similar activities *in vitro* and equivalent bioavailability (see Supplementary Material). On the basis of these results, racemate **14** was used for evaluation of *in vivo* antitumor efficacy in H1993 and SNU-5 xenograft models, respectively. As shown in **Fig. 3**, this compound demonstrated significant tumor growth inhibition in the treated groups of both subcutaneous xenograft models. The percent tumor growth inhibition (%TGI) at 3-week in the H1993 xenograft model was 55.5%, 78.7%, and 90.8% at doses of 0.1, 1, and 10 mg/kg, respectively. In the SNU-5 xenograft model, the percent tumor regression value (%PTR) at 2-week was 34.0%, 79.2%, and 87.9% at doses of 0.3, 1, and 3 mg/kg, respectively. During the experiment, none of mice in all the dosing groups displayed body weight loss or apparent toxicity.

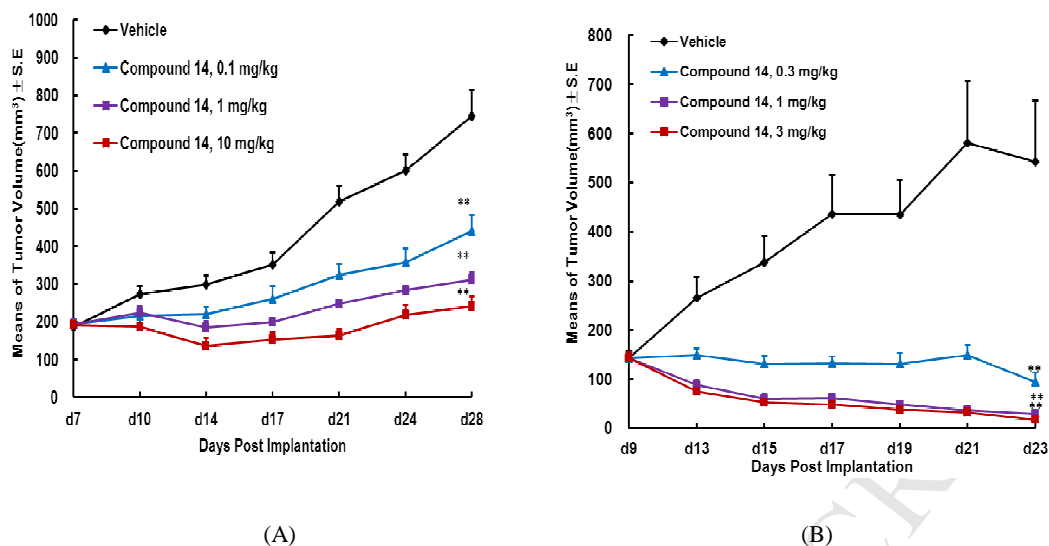


Fig. 3. (A) Growth inhibition of **14** in H1993 xenograft model in mice. Mice bearing H1993 tumors were orally administered **14** once daily at the indicated dose levels or vehicle alone for 3 weeks. (B) Growth inhibition of **14** in SNU-5 xenograft model in mice. Mice bearing SNU-5 tumors were orally administered **14** once daily at the indicated dose levels or vehicle alone for 2 weeks. Data represents the mean \pm SEM. for each group over the treatment period (n=6-7).

2.3. Molecular docking study

In this study, compound **14** was docked into the active site of c-Met kinase to obtain detailed information. This compound adopts a bent “U-shaped” conformation binding mode and is bound to the activation loop of c-Met kinase in the same way as most second generations of c-Met

inhibitors. As illustrated in **Fig. 4**, all the important interactions with the kinase which were reported by several publications were retained [15, 17, 21, 25, 27]: (1) a hydrogen bond between Met-1160 and nitrogen atom of quinoline moiety (hinge binder); (2) a π - π stacking interaction between Tyr-1159 and the quinoline ring; (3) a hydrogen bond interaction between the *N*-H of Asp-1222 residue and *N*-3 nitrogen of the fused ring; (4) a π - π stacking interaction between Tyr-1230 and the large coplanar structure of triazolopyrazine core with the side chain at 6-position. In addition to these classical interactions, the *N*-hydroxyethyl-pyrazol-4-yl group was directed toward the solvent-accessible region of c-Met, forming hydrogen bond network with Tyr-1230 and Arg-1086 via a water molecule; and the hydroxyl group forms hydrogen-bonding interaction with Asp-1231. It indicated that there is a halogen bond interaction between 7-F and nitrogen atom at the 2-position of core ring (displayed as blue dashed line) which is beneficial to the stability of binding conformation. Besides, we think the scaffold of triazolopyrazine which showed more electron deficiency than imidazopyrazine may lead to a stronger π - π stacking interaction with Tyr-1230. All above interactions contribute to the better ligand efficiency against c-Met.

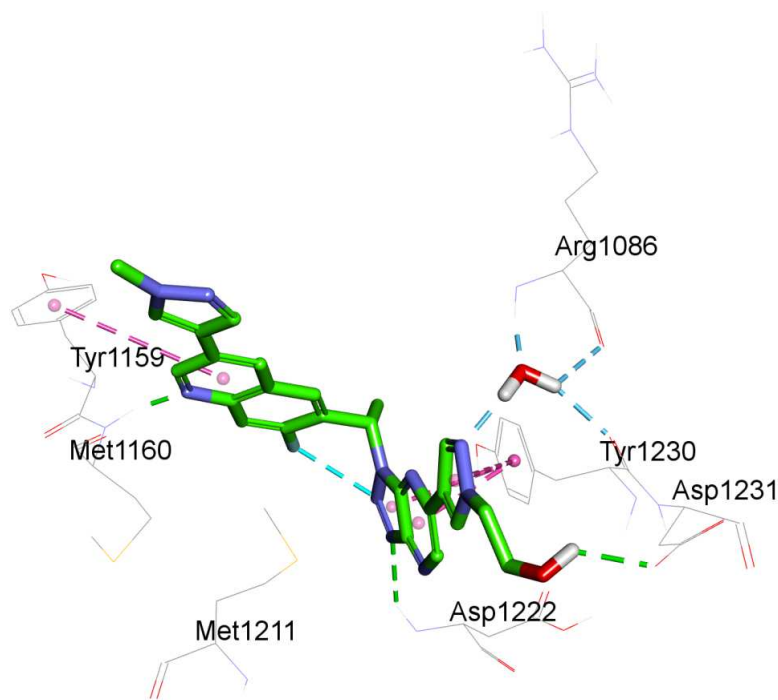


Fig. 4. Compound **14** was docked into the active site of c-Met.

3. Conclusions

In summary, what described here is the rationally guided optimization of a series of 3-substituted-6-(1-(1*H*-[1,2,3]triazolo[4,5-*b*]pyrazin-1-yl)ethyl)quinoline derivatives through metabolite profiling-based structural modification of lead compound **1** in order to improve the ADME properties. By means of bioisosteric replacement, metabolically stable [1,2,3]triazolo[4,5-*b*]pyrazine ring was selected as the core ring. Large substituents were attached to the 2-position or 3-position of quinoline moiety with the hope of increasing metabolic stability. Among them, 3-substituted compounds not only exhibited potent inhibitory activities *in vitro*, but also were stable in liver microsomes among different species. Further SAR investigation revealed that the introduction of *N*-methyl-1*H*-pyrazol-4-yl group at the 3-position of quinoline moiety is favorable for achieving a better potency in both enzymatic and cellular assays. Different from our

earlier SAR, the effect of fluorine atom at 7-position or 5, 7-position of quinoline moiety and substituents at 6-position of triazolo[4,5-*b*]pyrazine core on the overall activity is not very significant. Racemate **14** demonstrated favorable pharmacokinetic properties *in vivo*, no significant AO metabolism, and excellent antitumor efficacy in c-Met overexpressed H1993 and SNU-5 xenograft models. Molecular docking analysis of **14** indicated this molecule assumed a “U-shaped” conformation binding mode, which is the typical character of selective c-Met inhibitor. Besides the well-known important interactions, the hydrogen bond network with Tyr-1230 and Arg-1086, the hydrogen bond interactions with Asp-1231 and the intramolecular halogen bond may be strong supplements to the binding with kinase. These docking results may provide additional insights into the protein-ligand interactions and potential structural modifications for further activity improvement. **14** was selected as a candidate for further development and this work is in progress.

4. Experimental

4.1. Chemistry

4.1.1. General

All reagents and solvents employed were purchased from commercial sources and used without further purification. Reactions were followed by thin-layer chromatography (TLC) using HSGF 254 silica-gel plates (0.15-0.2 mm thickness) and visualized with UV light (254 nm). Silica-gel chromatography was done using the appropriate size Biotage prepacked silica filled cartridges.

Melting points were determined using a Shenguang WRR digital apparatus, and were uncorrected. NMR data were recorded on a *Bruker* 400 MHz Digital NMR Spectrometer using CDCl_3 or $\text{DMSO-}d_6$ as solvents. Chemical shifts are expressed as δ units (in NMR description, s, singlet; d, doublet; t, triplet; q, quartet; m, multiplet; dd, double doublet; and brs, broad singlet). All coupling constants (J) are reported in Hertz (Hz). High resolution mass spectra were measured with a Waters Synapt G2-S Q-ToF spectrometer using an ESI source coupled to a Waters Acquity UPLC system.

4.1.2. General synthetic procedure of title compounds **2-26**

To a solution of **d1-d7** (1 equiv., synthetic procedures see supplementary material) in the mixture of dioxane/ H_2O (4:1, v/v), corresponding boric acid or boric acid ester (1.5 equiv.), $\text{Pd}(\text{dppf})_2\text{Cl}_2 \cdot \text{DCM}$ complex (0.05 equiv.), and K_2CO_3 (3 equiv.) were added. The reaction mixture was bubbled with N_2 for 2 min and then stirred at 110°C for 4h. The mixture was concentrated and purified by flash column chromatography to afford the corresponding title compounds **2-26**.

4.1.2.1.

2-(1-Methyl-1H-pyrazol-4-yl)-6-(1-(6-(1-methyl-1H-pyrazol-4-yl)-1H-[1,2,3]triazolo[4,5-b]pyrazin-1-yl)ethyl)quinoline (2). Yellow solid. Yield: 57%. Mp: $168\text{-}170^\circ\text{C}$. ^1H NMR (400 MHz, $\text{DMSO-}d_6$) δ 9.17 (s, 1H), 8.61 (s, 1H), 8.44 (s, 1H), 8.33 (d, $J=8.8$ Hz, 1H), 8.27 (s, 1H), 8.13 (s, 1H), 7.99 (s, 1H), 7.91 (d, $J=8.8$ Hz, 1H), 7.83-7.80 (m, 2H), 6.54 (q, $J=7.2$ Hz, 1H), 3.94 (s, 3H), 3.90 (s, 3H), 2.24 (d, $J=7.2$ Hz, 3H). ^{13}C NMR (100 MHz, $\text{DMSO-}d_6$) δ 152.77, 148.42, 147.72, 147.60, 142.43, 138.91, 138.24, 137.91, 137.50, 137.35, 132.04, 130.99, 129.32, 128.99, 126.60,

126.11, 123.32, 119.82, 119.75, 57.95, 39.44, 39.26, 20.70. HRMS (ESI): $[M+H]^+=437.1953$, $C_{23}H_{20}N_{10}$ calcd for 436.1872; retention time 1.99 min, >95% pure.

4.1.2.2.

2-Fluoro-N-methyl-4-(1-(1-(2-(1-methyl-1H-pyrazol-4-yl)quinolin-6-yl)ethyl)-1H-[1,2,3]triazolo[4,5-b]pyrazin-6-yl)benzamide (3). Intermediate methyl 2-fluoro-4-(1-(1-(2-(1-methyl-1H-pyrazol-4-yl)quinolin-6-yl)ethyl)-1H-[1,2,3]triazolo[4,5-b]pyrazin-6-yl)benzoate was prepared by the general procedure using methyl 2-fluoro-4-(4,4,5,5-tetramethyl-1,3,2-dioxaborolan-2-yl)benzoate as the reagent. This intermediate (30 mg, 0.06 mmol) was added into methanamine solution (33% in alcohol, 10ml). The mixture was stirred at rt for 3h. Evaporated the solvent and the residue was purified by column chromatography to give the title compound as yellow solid. Yield: 30%. Mp: 245-247°C. 1H NMR (400 MHz, $DMSO-d_6$) δ 9.56 (s, 1H), 8.45 (s, 1H), 8.40 (brs, 1H), 8.35 (d, $J=8.4$ Hz, 1H), 8.23-8.20 (m, 2H), 8.14 (s, 1H), 8.06 (s, 1H), 7.93 (d, $J=8.4$ Hz, 1H), 7.87-7.81 (m, 3H), 6.71 (q, $J=7.2$ Hz, 1H), 3.92 (s, 3H), 2.82 (d, $J=4.4$ Hz, 3H), 2.28 (d, $J=7.2$ Hz, 3H). ^{13}C NMR (100 MHz, $DMSO-d_6$) δ 163.90, 161.17, 158.70, 152.82, 149.99, 148.89, 147.76, 142.90, 139.50, 139.42, 138.25, 137.78, 137.34, 137.28, 131.45, 131.42, 131.00, 129.34, 129.06, 126.60, 126.28, 124.21, 124.18, 123.32, 119.77, 115.90, 115.66, 58.25, 39.26, 26.76, 20.85. HRMS (ESI): $[M+H]^+=508.2012$, $C_{27}H_{22}FN_9O$ calcd for 507.1931; retention time 2.11 min, >95% pure.

4.1.2.3.

4-(1-(1-(2-(1-Methyl-1H-pyrazol-4-yl)quinolin-6-yl)ethyl)-1H-[1,2,3]triazolo[4,5-b]pyrazin-6-yl)

aniline (4). Yellow solid. Yield: 52%. Mp: 275-277°C. ¹H NMR (400 MHz, DMSO-*d*₆) δ 9.28 (s, 1H), 8.45 (s, 1H), 8.34 (d, *J*=8.4 Hz, 1H), 8.14 (s, 1H), 8.04 (d, *J*=8.4 Hz, 2H), 7.99 (d, *J*=1.2 Hz, 1H), 7.92 (d, *J*=8.4 Hz, 1H), 7.83 (d, *J*=8.8 Hz, 1H), 7.82 (dd, *J*₁=8.8 Hz, *J*₂=2.0 Hz, 1H), 6.70 (d, *J*=8.4 Hz, 2H), 6.58 (q, *J*=7.2 Hz, 1H), 5.90 (s, 2H), 3.91 (s, 3H), 2.24 (d, *J*=7.2 Hz, 3H). ¹³C NMR (100 MHz, DMSO-*d*₆) δ 152.96, 152.74, 152.48, 147.71, 147.44, 141.89, 138.24, 137.97, 137.70, 137.32, 130.99, 129.76, 129.31, 128.98, 126.60, 126.04, 123.34, 122.30, 119.73, 114.34, 57.73, 39.26, 20.82. HRMS (ESI): [M+H]⁺=448.1988, C₂₅H₂₁N₉ calcd for 447.1920; retention time 2.11 min, >95% pure.

4.1.2.4.

3-(1-Methyl-1H-pyrazol-4-yl)-6-(1-(6-(1-methyl-1H-pyrazol-4-yl)-1H-[1,2,3]triazolo[4,5-b]pyrazin-1-yl)ethyl)quinoline (5). Yellow solid. Yield: 62%. Mp: 230-232°C. ¹H NMR (400 MHz, DMSO-*d*₆) δ 9.20 (s, 1H), 9.18 (d, *J*=2.4 Hz, 1H), 8.63 (s, 1H), 8.49 (d, *J*=2.0 Hz, 1H), 8.38 (s, 1H), 8.29 (s, 1H), 8.08 (s, 1H), 8.00 (d, *J*=8.8 Hz, 1H), 7.91 (d, *J*=2.0 Hz, 1H), 7.82 (dd, *J*₁=8.4 Hz, *J*₂=2.0 Hz, 1H), 6.59 (q, *J*=6.8 Hz, 1H), 3.95 (s, 3H), 3.92 (s, 3H), 2.27 (d, *J*=6.8 Hz, 3H). HRMS (ESI): [M+H]⁺=437.1951, C₂₃H₂₀N₁₀ calcd for 436.1872; retention time 2.09 min, >95% pure.

4.1.2.5.

3-(4-Fluorophenyl)-6-(1-(6-(1-methyl-1H-pyrazol-4-yl)-1H-[1,2,3]triazolo[4,5-b]pyrazin-1-yl)ethyl)quinoline (6). Yellow solid. Yield: 25%. Mp: 196-198°C. ¹H NMR (400 MHz, DMSO-*d*₆) δ 9.23 (d, *J*=2.0 Hz, 1H), 9.20 (s, 1H), 8.66 (d, *J*=2.4 Hz, 1H), 8.63 (s, 1H), 8.29 (s, 1H), 8.06 (d, *J*=8.8

Hz, 1H), 8.05 (s, 1H), 7.95-7.90 (m, 3H), 7.38 (t, $J=8.8$ Hz, 2H), 6.60 (q, $J=6.8$ Hz, 1H), 3.94 (s, 3H), 2.28 (d, $J=6.8$ Hz, 3H). ^{13}C NMR (100 MHz, DMSO- d_6) δ 164.06, 161.62, 150.27, 148.47, 147.62, 146.73, 142.46, 139.27, 138.92, 137.98, 133.84, 133.81, 133.51, 132.67, 132.04, 129.80, 129.72, 128.86, 127.84, 126.39, 119.80, 116.66, 116.44, 57.95, 39.44, 20.73. HRMS (ESI): $[\text{M}+\text{H}]^+=451.1831$, $\text{C}_{25}\text{H}_{19}\text{FN}_8$ calcd for 450.1717; retention time 2.71 min, >95% pure.

4.1.2.6.

*2-Fluoro-4-(1-(1-(3-(4-fluorophenyl)quinolin-6-yl)ethyl)-1H-[1,2,3]triazolo[4,5-*b*]pyrazin-6-yl)-N-methylbenzamide (7)*. This compound was prepared as a yellow solid by a procedure similar to that described for the synthesis of compound **3** using methyl 2-fluoro-4-(1-(1-(3-(4-fluorophenyl)quinolin-6-yl)ethyl)-1H-[1,2,3]triazolo[4,5-*b*]pyrazin-6-yl)benzoate as a starting material. Yield: 51%. Mp: 188-190°C. ^1H NMR (400 MHz, DMSO- d_6) δ 9.58 (s, 1H), 9.23 (d, $J=2.0$ Hz, 1H), 8.66 (d, $J=2.0$ Hz, 1H), 8.39 (brs, 1H), 8.22 (s, 1H), 8.21-8.18 (m, 1H), 8.12 (d, $J=1.2$ Hz, 1H), 8.07 (d, $J=8.8$ Hz, 1H), 7.96-7.91 (m, 3H), 7.82 (t, $J=8.0$ Hz, 1H), 7.38 (t, $J=8.8$ Hz, 2H), 6.77 (q, $J=7.2$ Hz, 1H), 2.82 (d, $J=4.8$ Hz, 3H), 2.30 (d, $J=7.2$ Hz, 3H). ^{13}C NMR (100 MHz, DMSO- d_6) δ 164.06, 163.88, 161.62, 161.17, 158.69, 150.31, 150.04, 150.02, 148.90, 146.76, 142.92, 139.48, 139.39, 139.09, 137.85, 133.83, 133.80, 133.49, 132.70, 131.46, 131.43, 129.80, 129.72, 128.92, 127.84, 126.51, 126.33, 126.18, 124.21, 124.18, 116.66, 116.44, 115.90, 115.66, 58.21, 26.76, 20.91. HRMS (ESI): $[\text{M}+\text{H}]^+=522.1851$, $\text{C}_{29}\text{H}_{21}\text{F}_2\text{N}_7\text{O}$ calcd for 521.1776; retention time 2.78 min, >95% pure.

4.1.2.7.

3-(4-Fluorophenyl)-6-(1-(6-(pyridin-4-yl)-1H-[1,2,3]triazolo[4,5-b]pyrazin-1-yl)ethyl)quinoline

(8). Yield: 59%. Mp: 199-201°C. ¹H NMR (400 MHz, DMSO-*d*₆) δ 9.61 (s, 1H), 9.23 (d, *J*=2.4 Hz, 1H), 8.82 (d, *J*=6.0 Hz, 2H), 8.66 (d, *J*=2.0 Hz, 1H), 8.24 (d, *J*=6.0 Hz, 2H), 8.11 (d, *J*=1.6 Hz, 1H), 8.07 (d, *J*=8.8 Hz, 1H), 7.96-7.90 (m, 3H), 7.38 (t, *J*=8.8 Hz, 2H), 6.77 (q, *J*=7.2 Hz, 1H), 2.32 (d, *J*=7.2 Hz, 3H). ¹³C NMR (100 MHz, DMSO-*d*₆) δ 164.05, 161.61, 151.16, 150.31, 149.77, 149.33, 146.76, 142.92, 142.75, 139.04, 137.97, 133.81, 133.78, 133.49, 132.68, 129.83, 129.79, 129.70, 128.86, 127.84, 126.48, 122.09, 116.65, 116.44, 58.40, 20.84. HRMS (ESI): [M+H]⁺=448.1687, C₂₆H₁₈FN₇ calcd for 447.1608; retention time 2.62 min, >95% pure.

4.1.2.8.

2-(4-(1-(1-(3-(1-Methyl-1H-pyrazol-4-yl)quinolin-6-yl)ethyl)-1H-[1,2,3]triazolo[4,5-b]pyrazin-6-yl)-1H-pyrazol-1-yl)ethan-1-ol (9). Yellow solid. Yield: 56%. Mp: 131-133°C. ¹H NMR (400 MHz, DMSO-*d*₆) δ 9.22 (s, 1H), 9.18 (d, *J*=2.0 Hz, 1H), 8.64 (s, 1H), 8.49 (d, *J*=1.6 Hz, 1H), 8.38 (s, 1H), 8.32 (s, 1H), 8.08 (s, 1H), 8.00 (d, *J*=8.8 Hz, 1H), 7.92 (d, *J*=1.6 Hz, 1H), 7.82 (dd, *J*₁=8.8 Hz, *J*₂=2.0 Hz, 1H), 6.60 (q, *J*=7.2 Hz, 1H), 4.98 (t, *J*=5.2 Hz, 1H), 4.25 (t, *J*=5.6 Hz, 2H), 3.92 (s, 3H), 3.80 (q, *J*=5.2 Hz, 2H), 2.26 (d, *J*=7.2 Hz, 3H). ¹³C NMR (100 MHz, DMSO-*d*₆) δ 149.70, 148.58, 147.59, 146.07, 142.50, 139.20, 138.95, 137.98, 137.05, 131.95, 130.07, 129.86, 129.06, 128.19, 127.81, 126.87, 125.65, 119.52, 119.05, 60.23, 57.86, 55.06, 39.27, 20.79. HRMS (ESI): [M+H]⁺=467.2069, C₂₄H₂₂N₁₀O calcd for 466.1978; retention time 1.94 min, >95% pure.

4.1.2.9.

2-Fluoro-4-(1-(1-(3-(1-methyl-1H-pyrazol-4-yl)quinolin-6-yl)ethyl)-1H-[1,2,3]triazolo[4,5-b]pyra

zin-6-yl)benzamide (10). Intermediate methyl

2-fluoro-4-(1-(1-(3-(1-methyl-1*H*-pyrazol-4-yl)quinolin-6-yl)ethyl)-1*H*-[1,2,3]triazolo[4,5-*b*]pyrazin-6-yl)benzoate (30 mg, 0.06 mmol) was added into ammonia solution (7 M in methanol, 10ml). The mixture was heated to 50°C overnight in a sealed tube. Evaporated the solvent and the residue was purified by column chromatography to give the title compound as yellow solid. Yield: 62%. Mp: 258-260°C. ¹H NMR (400 MHz, DMSO-*d*₆) δ 9.58 (s, 1H), 9.18 (d, *J*=2.0 Hz, 1H), 8.50 (d, *J*=2.0 Hz, 1H), 8.38 (s, 1H), 8.22-8.18 (m, 2H), 8.08 (s, 1H), 8.00 (d, *J*=8.8 Hz, 1H), 7.99 (s, 1H), 7.88-7.84 (m, 3H), 7.78 (s, 1H), 6.74 (q, *J*=7.2 Hz, 1H), 3.92 (s, 3H), 2.29 (d, *J*=7.2 Hz, 3H). ¹³C NMR (100 MHz, DMSO-*d*₆) δ 165.12, 161.30, 158.82, 150.14, 150.12, 148.91, 144.21, 143.01, 141.66, 139.49, 139.41, 137.91, 137.86, 137.54, 137.40, 131.89, 131.56, 131.53, 130.13, 129.11, 128.18, 126.30, 126.15, 124.16, 124.13, 123.06, 117.11, 115.93, 115.68, 57.83, 39.45, 20.80. HRMS (ESI): [M+H]⁺=494.1848, C₂₆H₂₀FN₉O calcd for 493.1775; retention time 2.11 min, >95% pure.

4.1.2.10.

2-Fluoro-*N*-methyl-4-(1-(1-(3-(1-methyl-1*H*-pyrazol-4-yl)quinolin-6-yl)ethyl)-1*H*-[1,2,3]triazolo[4,5-*b*]pyrazin-6-yl)benzamide (11). This compound was prepared as a yellow solid by a procedure similar to that described for the synthesis of compound 3 using methyl 2-fluoro-4-(1-(1-(3-(1-methyl-1*H*-pyrazol-4-yl)quinolin-6-yl)ethyl)-1*H*-[1,2,3]triazolo[4,5-*b*]pyrazin-6-yl)benzoate as a starting material. Yield: 67%. Mp: 132-134°C. ¹H NMR (400 MHz, DMSO-*d*₆) δ 9.57 (s, 1H), 9.17 (d, *J*=1.6 Hz, 1H), 8.49 (s, 1H), 8.39 (s, 1H), 8.37 (s, 1H), 8.21 (s, 1H), 8.19 (d, *J*=2.0 Hz, 1H), 8.07 (s, 1H), 8.00-7.98 (m, 2H), 7.86-7.80 (m, 2H), 6.74 (q, *J*=6.8 Hz,

1H), 3.91 (s, 3H), 2.82 (d, $J=4.4$ Hz, 3H), 2.28 (d, $J=6.8$ Hz, 3H). HRMS (ESI): $[M+H]^+=508.2007$, $C_{27}H_{22}FN_9O$ calcd for 507.1931; retention time 2.21 min, >95% pure.

4.1.2.11.

3-(1-Methyl-1H-pyrazol-4-yl)-6-(1-(6-(pyridin-4-yl)-1H-[1,2,3]triazolo[4,5-b]pyrazin-1-yl)ethyl)quinoline (12). Yellow solid. Yield: 35%. Mp: 210-212°C. 1H NMR (400 MHz, DMSO- d_6) δ 9.60 (s, 1H), 9.17 (d, $J=2.4$ Hz, 1H), 8.82 (dd, $J_1=4.8$ Hz, $J_2=1.6$ Hz, 2H), 8.49 (d, $J=2.0$ Hz, 1H), 8.38 (s, 1H), 8.24 (dd, $J_1=4.8$ Hz, $J_2=1.6$ Hz, 2H), 8.08 (s, 1H), 8.00 (d, $J=8.4$ Hz, 1H), 7.97 (d, $J=1.6$ Hz, 1H), 7.85 (dd, $J_1=8.8$ Hz, $J_2=2.0$ Hz, 1H), 6.74 (q, $J=6.8$ Hz, 1H), 3.91 (s, 3H), 2.30 (d, $J=6.8$ Hz, 3H). ^{13}C NMR (100 MHz, DMSO- d_6) δ 151.15, 149.74, 149.31, 146.11, 142.91, 142.73, 138.91, 137.93, 137.03, 130.04, 129.91, 129.03, 128.19, 127.81, 126.88, 125.82, 122.08, 119.01, 58.40, 39.27, 20.85. HRMS (ESI): $[M+H]^+=434.1835$, $C_{24}H_{19}N_9$ calcd for 433.1763; retention time 1.98 min, >95% pure.

4.1.2.12.

7-Fluoro-3-(1-methyl-1H-pyrazol-4-yl)-6-(1-(6-(1-methyl-1H-pyrazol-4-yl)-1H-[1,2,3]triazolo[4,5-b]pyrazin-1-yl)ethyl)quinoline (13). Yellow solid. Yield: 56%. Mp: 228-230°C. 1H NMR (400 MHz, DMSO- d_6) δ 9.21 (d, $J=2.0$ Hz, 1H), 9.20 (s, 1H), 8.58 (s, 2H), 8.36 (s, 1H), 8.23 (s, 1H), 8.07 (d, $J=8.0$ Hz, 1H), 8.06 (s, 1H), 7.80 (d, $J=12.0$ Hz, 1H), 6.72 (q, $J=7.2$ Hz, 1H), 3.93 (s, 3H), 3.91 (s, 3H), 2.24 (d, $J=7.2$ Hz, 3H). HRMS (ESI): $[M+H]^+=455.1864$, $C_{23}H_{19}FN_{10}$ calcd for 454.1778; retention time 2.26 min, >95% pure.

4.1.2.13.

2-(4-(1-(1-(7-Fluoro-3-(1-methyl-1*H*-pyrazol-4-yl)quinolin-6-yl)ethyl)-1*H*-[1,2,3]triazolo[4,5-*b*]pyrazin-6-yl)-1*H*-pyrazol-1-yl)ethan-1-ol (**14**). Yellow solid. Yield: 49%. Mp: 158-160°C. ¹H NMR (400 MHz, DMSO-*d*₆) δ 9.22 (s, 1H), 9.20 (d, *J*=2.0 Hz, 1H), 8.60 (s, 1H), 8.58 (d, *J*=1.6 Hz, 1H), 8.36 (s, 1H), 8.26 (s, 1H), 8.09 (d, *J*=8.0 Hz, 1H), 8.06 (s, 1H), 7.79 (d, *J*=12.0 Hz, 1H), 6.74 (q, *J*=7.2 Hz, 1H), 4.96 (t, *J*=5.2 Hz, 1H), 4.24 (t, *J*=5.2 Hz, 2H), 3.92 (s, 3H), 3.78 (q, *J*=5.2 Hz, 2H), 2.25 (d, *J*=7.2 Hz, 3H). ¹³C NMR (100 MHz, DMSO-*d*₆) δ 161.11, 158.63, 150.74, 148.60, 147.47, 146.81, 146.69, 142.52, 138.89, 137.86, 136.98, 131.92, 130.29, 128.99, 128.91, 128.73, 128.32, 128.27, 126.45, 126.42, 125.51, 119.47, 118.86, 113.33, 113.13, 60.22, 55.04, 52.19, 39.28, 20.01. HRMS (ESI): [M+H]⁺=485.1949, C₂₄H₂₁FN₁₀O calcd for 484.1884; retention time 0.09 min, >95% pure.

4.1.2.14.

2-Fluoro-4-(1-(1-(7-fluoro-3-(1-methyl-1*H*-pyrazol-4-yl)quinolin-6-yl)ethyl)-1*H*-[1,2,3]triazolo[4,5-*b*]pyrazin-6-yl)benzamide (**15**). This compound was prepared as a yellow solid by a procedure similar to that described for the synthesis of compound **10** using methyl 2-fluoro-4-(1-(1-(7-fluoro-3-(1-methyl-1*H*-pyrazol-4-yl)quinolin-6-yl)ethyl)-1*H*-[1,2,3]triazolo[4,5-*b*]pyrazin-6-yl)benzoate as a starting material. Yield: 74%. Mp: 243-245°C. ¹H NMR (400 MHz, DMSO-*d*₆) δ 9.57 (s, 1H), 9.22 (d, *J*=2.4 Hz, 1H), 8.59 (d, *J*=2.4 Hz, 1H), 8.37 (s, 1H), 8.19 (d, *J*=8.4 Hz, 1H), 8.16 (d, *J*=8.4 Hz, 1H), 8.14 (d, *J*=12.0 Hz, 1H), 8.07 (s, 1H), 7.86-7.77 (m, 4H), 6.88 (q, *J*=7.2 Hz, 1H), 3.92 (s, 3H), 2.29 (d, *J*=7.2 Hz, 3H). ¹³C NMR (100 MHz, DMSO-*d*₆) δ 165.11, 162.35, 161.28, 159.82, 158.80, 150.09, 150.07, 148.79, 146.66, 143.01, 140.74, 140.60,

139.44, 139.36, 137.72, 137.30, 136.02, 131.55, 131.52, 130.66, 130.49, 129.77, 129.49, 129.44, 127.39, 127.38, 126.31, 126.26, 126.16, 124.10, 124.07, 117.46, 115.86, 115.61, 109.12, 108.88, 52.50, 39.42, 19.83. HRMS (ESI): $[M+H]^+$ =512.1761, $C_{26}H_{19}F_2N_9O$ calcd for 511.1681; retention time 2.26 min, >95% pure.

4.1.2.15.

2-Fluoro-4-(1-(1-(7-fluoro-3-(1-methyl-1H-pyrazol-4-yl)quinolin-6-yl)ethyl)-1H-[1,2,3]triazolo[4,5-b]pyrazin-6-yl)-N-methylbenzamide (16). This compound was prepared as a yellow solid by a procedure similar to that described for the synthesis of compound **3** using methyl 2-fluoro-4-(1-(1-(7-fluoro-3-(1-methyl-1H-pyrazol-4-yl)quinolin-6-yl)ethyl)-1H-[1,2,3]triazolo[4,5-b]pyrazin-6-yl)benzoate as a starting material. Yield: 80%. Mp: 226-228°C. 1H NMR (400 MHz, $DMSO-d_6$) δ 9.58 (s, 1H), 9.23 (s, 1H), 8.60 (s, 1H), 8.38 (s, 2H), 8.20-8.13 (m, 3H), 8.08 (s, 1H), 7.82-7.79 (m, 2H), 6.88 (q, $J=6.8$ Hz, 1H), 3.93 (s, 3H), 2.82 (d, $J=4.4$ Hz, 3H), 2.30 (d, $J=6.8$ Hz, 3H). HRMS (ESI): $[M+H]^+$ =526.1915, $C_{27}H_{21}F_2N_9O$ calcd for 525.1837; retention time 2.36 min, >95% pure.

4.1.2.16.

7-Fluoro-3-(1-methyl-1H-pyrazol-4-yl)-6-(1-(6-(pyridin-4-yl)-1H-[1,2,3]triazolo[4,5-b]pyrazin-1-yl)ethyl)quinoline (17). Yellow solid. Yield: 65%. Mp: 227-229°C. 1H NMR (400 MHz, $DMSO-d_6$) δ 9.60 (s, 1H), 9.20 (d, $J=2.0$ Hz, 1H), 8.80 (d, $J=6.0$ Hz, 2H), 8.58 (d, $J=1.6$ Hz, 1H), 8.36 (s, 1H), 8.18 (d, $J=6.0$ Hz, 2H), 8.16 (d, $J=8.4$ Hz, 1H), 8.06 (s, 1H), 7.79 (d, $J=12.0$ Hz, 1H), 6.88 (q, $J=6.8$ Hz, 1H), 3.91 (s, 3H), 2.30 (d, $J=6.8$ Hz, 3H). ^{13}C NMR (100 MHz, $DMSO-d_6$) δ 161.13,

158.65, 151.16, 150.82, 149.73, 149.22, 146.88, 146.75, 142.95, 142.68, 137.82, 136.97, 130.27, 128.99, 128.59, 128.53, 128.49, 128.42, 126.47, 126.45, 125.53, 122.02, 118.84, 113.40, 113.19, 52.75, 52.72, 39.29, 19.98. HRMS (ESI): $[M+H]^+=452.1744$, $C_{24}H_{18}FN_9$ calcd for 451.1669; retention time 2.14 min, >95% pure.

4.1.2.17.

5,7-Difluoro-3-(1-methyl-1H-pyrazol-4-yl)-6-(1-(6-(1-methyl-1H-pyrazol-4-yl)-1H-[1,2,3]triazolo[4,5-b]pyrazin-1-yl)ethyl)quinoline (18). Yellow solid. Yield: 95%. Mp: 172-174°C. 1H NMR (400 MHz, DMSO- d_6) δ 9.30 (d, $J=2.0$ Hz, 1H), 9.15 (s, 1H), 8.61 (d, $J=1.2$ Hz, 1H), 8.50 (s, 1H), 8.48 (s, 1H), 8.20 (s, 1H), 8.08 (s, 1H), 7.74 (d, $J=11.6$ Hz, 1H), 6.76 (q, $J=7.2$ Hz, 1H), 3.92 (s, 6H), 2.38 (d, $J=7.2$ Hz, 3H). ^{13}C NMR (100 MHz, DMSO- d_6) δ 161.08, 160.99, 158.60, 158.51, 157.55, 157.45, 154.97, 154.87, 151.97, 148.14, 147.46, 146.12, 146.07, 145.98, 145.93, 142.22, 138.61, 138.03, 137.30, 131.73, 129.47, 126.95, 122.86, 119.74, 118.51, 116.38, 116.22, 114.49, 114.35, 114.29, 114.14, 110.05, 110.01, 109.83, 109.79, 49.90, 39.28, 18.56. HRMS (ESI): $[M+H]^+=473.1766$, $C_{23}H_{18}F_2N_{10}$ calcd for 472.1684; retention time 2.38 min, >95% pure.

4.1.2.18.

2-(4-(1-(1-(5,7-Difluoro-3-(1-methyl-1H-pyrazol-4-yl)quinolin-6-yl)ethyl)-1H-[1,2,3]triazolo[4,5-b]pyrazin-6-yl)-1H-pyrazol-1-yl)ethan-1-ol (19). Yellow solid. Yield: 70%. Mp: 210-212°C. 1H NMR (400 MHz, DMSO- d_6) δ 9.30 (d, $J=1.6$ Hz, 1H), 9.17 (s, 1H), 8.59 (s, 1H), 8.51 (s, 1H), 8.48 (s, 1H), 8.19 (s, 1H), 8.10 (s, 1H), 7.72 (d, $J=12.0$ Hz, 1H), 6.78 (q, $J=7.2$ Hz, 1H), 4.96 (t, $J=5.2$ Hz, 1H), 4.22 (t, $J=5.2$ Hz, 2H), 3.92 (s, 3H), 3.77 (q, $J=5.2$ Hz, 2H), 2.37 (d, $J=7.2$ Hz, 3H).

^{13}C NMR (100 MHz, $\text{DMSO-}d_6$) δ 161.12, 161.02, 158.63, 158.54, 157.56, 157.46, 154.98, 154.88, 152.00, 148.27, 147.46, 146.14, 146.09, 145.99, 145.94, 142.26, 138.66, 138.05, 137.32, 131.70, 129.50, 126.98, 122.90, 119.45, 118.52, 116.39, 116.23, 114.53, 114.38, 114.32, 114.17, 110.06, 110.02, 109.84, 109.80, 60.19, 55.05, 49.89, 39.29, 18.58. HRMS (ESI): $[\text{M}+\text{H}]^+=503.1872$, $\text{C}_{24}\text{H}_{20}\text{F}_2\text{N}_{10}\text{O}$ calcd for 502.1790; retention time 2.21 min, >95% pure.

4.1.2.19.

4-(1-(1-(5,7-Difluoro-3-(1-methyl-1H-pyrazol-4-yl)quinolin-6-yl)ethyl)-1H-[1,2,3]triazolo[4,5-b]pyrazin-6-yl)-2-fluorobenzamide (20). This compound was prepared as a yellow solid by a procedure similar to that described for the synthesis of compound **10** using methyl 4-(1-(1-(5,7-difluoro-3-(1-methyl-1H-pyrazol-4-yl)quinolin-6-yl)ethyl)-1H-[1,2,3]triazolo[4,5-b]pyrazin-6-yl)-2-fluorobenzoate as a starting material. Yield: 52%. Mp: 254-256°C. ^1H NMR (400 MHz, $\text{DMSO-}d_6$) δ 9.54 (s, 1H), 9.31 (d, $J=2.0$ Hz, 1H), 8.60 (d, $J=2.0$ Hz, 1H), 8.49 (s, 1H), 8.19 (s, 1H), 8.07 (dd, $J_1=8.0$ Hz, $J_2=1.6$ Hz, 1H), 8.00 (dd, $J_1=12.0$ Hz, $J_2=1.2$ Hz, 1H), 7.83 (brs, 1H), 7.81-7.73 (m, 3H), 6.88 (q, $J=7.2$ Hz, 1H), 3.92 (s, 3H), 2.42 (d, $J=7.2$ Hz, 3H). HRMS (ESI): $[\text{M}+\text{H}]^+=530.1666$, $\text{C}_{26}\text{H}_{18}\text{F}_3\text{N}_9\text{O}$ calcd for 529.1586; retention time 2.37 min, >95% pure.

4.1.2.20.

4-(1-(1-(5,7-Difluoro-3-(1-methyl-1H-pyrazol-4-yl)quinolin-6-yl)ethyl)-1H-[1,2,3]triazolo[4,5-b]pyrazin-6-yl)-2-fluoro-N-methylbenzamide (21). This compound was prepared as a yellow solid by a procedure similar to that described for the synthesis of compound **3** using methyl 4-(1-(1-(5,7-difluoro-3-(1-methyl-1H-pyrazol-4-yl)quinolin-6-yl)ethyl)-1H-[1,2,3]triazolo[4,5-b]p

pyrazin-6-yl)-2-fluorobenzoate as a starting material. Yield: 33%. Mp: >280°C. ¹H NMR (400 MHz, DMSO-*d*₆) δ 9.53 (s, 1H), 9.30 (d, *J*=2.0 Hz, 1H), 8.59 (d, *J*=2.0 Hz, 1H), 8.48 (s, 1H), 8.36 (brs, 1H), 8.18 (s, 1H), 8.06 (dd, *J*₁=8.0 Hz, *J*₂=1.6 Hz, 1H), 8.00 (dd, *J*₁=11.6 Hz, *J*₂=1.2 Hz, 1H), 7.77-7.72 (m, 2H), 6.88 (q, *J*=6.8 Hz, 1H), 3.91 (s, 3H), 2.80 (d, *J*=4.8 Hz, 3H), 2.41 (d, *J*=6.8 Hz, 3H). HRMS (ESI): [M+H]⁺=544.1816, C₂₇H₂₀F₃N₉O calcd for 543.1743; retention time 2.46 min, >95% pure.

4.1.2.21.

5,7-Difluoro-3-(1-methyl-1H-pyrazol-4-yl)-6-(1-(6-(pyridin-4-yl)-1H-[1,2,3]triazolo[4,5-*b*]pyrazin-1-yl)ethyl)quinoline (**22**). Yellow solid. Yield: 60%. Mp: 219-221°C. ¹H NMR (400 MHz, CDCl₃) δ 9.26 (s, 1H), 9.12 (d, *J*=2.0 Hz, 1H), 8.81 (d, *J*=6.4 Hz, 2H), 8.36 (d, *J*=2.0 Hz, 1H), 7.93-7.92 (m, 3H), 7.82 (s, 1H), 7.64 (d, *J*=11.2 Hz, 1H), 6.87 (q, *J*=7.2 Hz, 1H), 4.03 (s, 3H), 2.54 (d, *J*=7.2 Hz, 3H). ¹³C NMR (100 MHz, DMSO-*d*₆) δ 161.07, 160.98, 158.58, 158.50, 157.68, 157.58, 155.11, 155.01, 152.07, 151.13, 149.36, 149.24, 146.20, 146.15, 146.06, 146.01, 142.74, 142.64, 138.02, 137.33, 129.51, 127.01, 122.90, 122.87, 121.80, 118.49, 116.44, 116.27, 114.29, 114.14, 114.08, 113.93, 110.16, 110.12, 109.95, 109.90, 50.32, 39.30, 18.51. HRMS (ESI): [M+H]⁺=470.1649, C₂₄H₁₇F₂N₉ calcd for 469.1575; retention time 2.26 min, >95% pure.

4.1.2.22.

7-Fluoro-3-(4-fluorophenyl)-6-(1-(6-(1-methyl-1H-pyrazol-4-yl)-1H-[1,2,3]triazolo[4,5-*b*]pyrazin-1-yl)ethyl)quinoline (**23**). Yellow solid. Yield: 61%. Mp: 202-204°C. ¹H NMR (400 MHz, CDCl₃) δ 9.12 (d, *J*=1.6 Hz, 1H), 8.92 (s, 1H), 8.24 (d, *J*=1.6 Hz, 1H), 8.12 (s, 1H), 8.07 (s, 1H), 7.91-7.88

(m, 2H), 7.62 (dd, $J_1=8.8$ Hz, $J_2=5.2$ Hz, 2H), 7.21 (t, $J=8.8$ Hz, 2H), 6.80 (q, $J=7.2$ Hz, 1H), 4.01 (s, 3H), 2.32 (d, $J=7.2$ Hz, 3H). ^{13}C NMR (100 MHz, DMSO- d_6) δ 164.07, 161.70, 161.62, 159.20, 151.29, 148.47, 147.61, 147.50, 142.46, 138.86, 137.85, 133.68, 133.63, 133.60, 132.21, 132.19, 132.01, 129.71, 129.63, 129.16, 129.11, 129.03, 128.86, 125.18, 119.75, 116.67, 116.46, 113.23, 113.02, 52.27, 39.39, 19.94. HRMS (ESI): $[\text{M}+\text{H}]^+=469.1718$, $\text{C}_{25}\text{H}_{18}\text{F}_2\text{N}_8$ calcd for 468.1622; retention time 2.85 min, >95% pure.

4.1.2.23.

7-Fluoro-3-(4-fluorophenyl)-6-(1-(6-(pyridin-4-yl)-1H-[1,2,3]triazolo[4,5-b]pyrazin-1-yl)ethyl)quinoline (24). Yellow solid. Yield: 54%. Mp: 234-235°C. ^1H NMR (400 MHz, DMSO- d_6) δ 9.62 (s, 1H), 9.28 (s, 1H), 8.81 (d, $J=5.2$ Hz, 2H), 8.77 (s, 1H), 8.33 (d, $J=8.4$ Hz, 1H), 8.21 (d, $J=5.2$ Hz, 2H), 7.94 (dd, $J_1=8.0$ Hz, $J_2=5.6$ Hz, 2H), 7.88 (d, $J=11.6$ Hz, 1H), 7.41 (t, $J=8.8$ Hz, 2H), 6.92 (q, $J=6.8$ Hz, 1H), 2.32 (d, $J=6.8$ Hz, 3H). ^{13}C NMR (100 MHz, DMSO- d_6) δ 164.08, 161.74, 161.64, 159.24, 151.40, 151.16, 149.76, 149.22, 147.67, 147.54, 142.96, 142.69, 137.85, 133.69, 133.63, 133.60, 132.26, 132.24, 129.73, 129.65, 129.32, 129.28, 128.79, 128.62, 125.21, 122.04, 116.71, 116.49, 113.30, 113.09, 52.78, 19.94. HRMS (ESI): $[\text{M}+\text{H}]^+=466.1591$, $\text{C}_{26}\text{H}_{17}\text{F}_2\text{N}_7$ calcd for 465.1513; retention time 2.76 min, >95% pure.

4.1.2.24.

5,7-Difluoro-3-(4-fluorophenyl)-6-(1-(6-(1-methyl-1H-pyrazol-4-yl)-1H-[1,2,3]triazolo[4,5-b]pyrazin-1-yl)ethyl)quinoline (25). Yellow solid. Yield: 33%. Mp: 203-205°C. ^1H NMR (400 MHz, DMSO- d_6) δ 9.35 (d, $J=2.0$ Hz, 1H), 9.14 (s, 1H), 8.73 (d, $J=2.0$ Hz, 1H), 8.48 (s, 1H), 8.09 (s,

1H), 7.99 (dd, $J_1=8.8$ Hz, $J_2=5.6$ Hz, 2H), 7.82 (d, $J=11.6$ Hz, 1H), 7.39 (t, $J=8.8$ Hz, 2H), 6.80 (q, $J=6.8$ Hz, 1H), 3.90 (s, 3H), 2.37 (d, $J=6.8$ Hz, 3H). ^{13}C NMR (100 MHz, DMSO- d_6) δ 164.25, 161.80, 161.71, 159.30, 159.21, 157.90, 157.80, 155.31, 155.21, 152.69, 148.17, 147.47, 146.91, 146.86, 146.76, 146.71, 142.24, 138.64, 138.03, 133.15, 133.12, 132.66, 131.76, 130.07, 129.98, 126.52, 126.49, 119.72, 116.67, 116.45, 116.02, 115.85, 114.68, 114.53, 114.47, 114.33, 110.02, 109.98, 109.80, 109.76, 49.85, 39.41, 18.54. HRMS (ESI): $[\text{M}+\text{H}]^+=487.1678$, $\text{C}_{25}\text{H}_{17}\text{F}_3\text{N}_8$ calcd for 486.1528; retention time 2.96 min, >95% pure.

4.1.2.25.

5,7-Difluoro-3-(4-fluorophenyl)-6-(1-(6-(pyridin-4-yl)-1H-[1,2,3]triazolo[4,5-b]pyrazin-1-yl)ethyl)quinoline (26). Yellow solid. Yield: 42%. Mp: 82-84°C. ^1H NMR (400 MHz, DMSO- d_6) δ 9.58 (s, 1H), 9.36 (d, $J=2.4$ Hz, 1H), 8.77 (dd, $J_1=4.4$ Hz, $J_2=1.6$ Hz, 2H), 8.73 (d, $J=1.6$ Hz, 1H), 8.11 (dd, $J_1=4.4$ Hz, $J_2=1.6$ Hz, 2H), 8.00 (dd, $J_1=8.8$ Hz, $J_2=1.6$ Hz, 2H), 7.84 (d, $J=11.6$ Hz, 1H), 7.40 (t, $J=8.8$ Hz, 2H), 6.93 (q, $J=7.2$ Hz, 1H), 2.43 (d, $J=7.2$ Hz, 3H). HRMS (ESI): $[\text{M}+\text{H}]^+=484.1551$, $\text{C}_{26}\text{H}_{16}\text{F}_3\text{N}_7$ calcd for 483.1419; retention time 2.88 min, >95% pure.

4.2. Biological protocols

4.2.1. In vitro enzymatic assay

Inhibition of test compound on c-Met kinase activity was determined by measuring the phosphorylation level of TK substrate-biotin peptide in a Homogenous Time-Resolved Fluorescence (HTRF) assay. Into a white 384-well plate was added 2 μL /well of 5X compound in

reaction buffer. Next, 4 μ L of reaction buffer (50 mM HEPES pH 7.0, 0.02% NaN_3 , 0.01% BSA, 0.1 mM Na_2VO_3 , 5 mM MgCl_2 and 1 mM DTT, containing 1 μ M TK substrate-biotin and 1 ng c-Met enzyme) was added to each well. After 5-10 min preincubation, the kinase reaction was initiated by the addition of 4 μ L of 18 μ M ATP in reaction buffer. After 30 minutes incubation at room temperature, the enzyme reaction was stopped by EDTA-containing buffer, which also contained europium-conjugated anti-phosphoresidue antibody and streptavidin-XL665 (SA-XL665) to allow for detection of the phosphorylated peptide product. Following 1 h incubation at room temperature fluorescence was measured with excitation of 337 nm and dual emission of 665 and 620 nm on Envision microplate reader (PerkinElmer). Signal was expressed in terms of HTRF ratio (fluorescence intensity at 665 nm/fluorescence intensity at 620 nm \times 10,000).

4.2.2. *In vitro* growth inhibition assay

NCI-H1993 cell line and SNU-5 cell line were purchased from the American Type Culture Collection (ATCC, Manassas, VA, USA). Cells were maintained in RPMI 1640 media and supplemented with 10% fetal bovine serum (Gibco Life Technologies, Grand Island, NY). NCI-H1993 cells were seeded at 5000 cells/well in 96-well plates and incubated overnight. On the next day, the cells were exposed to various concentrations of compounds and further cultured for 72 h. After chromogenic reaction with Cell Counting Kit-8 (CCK-8; Dojindo Laboratories, Kumamoto, Japan), the OD450 (with reference of OD650) was measured using a Flexstation 3 reader (Molecular Devices, USA). IC_{50} values were calculated using the GraphPad Prism Software. Each experiment was carried out thrice, each time in duplicate. The SNU-5 cell line assay was

operated in a similar procedure as NCI-H1993 assay.

4.2.3. Metabolic stability in human/ rat/monkey liver microsomes

This assay utilized a 150 μ l incubation system containing human or rat or monkey liver microsomes (0.5 mg/ml) to preincubate with 1 μ M test compound for 5 min at 37°C in 100 mM phosphate buffer (pH 7.4). The reactions were initiated by adding NADPH (1 mM). Midazolam was used as positive control. After 0, 5, 10 and 30 min incubations at 37°C, the reactions were stopped by adding 300 μ l acetonitrile containing tinidazole of 0.1 μ g/ml as internal standard. The samples were vortexed for 10 min, and then centrifuged at 6000 g for 10 min twice at 4°C and an aliquot of supernatant was sampled for LC-MS/MS analysis. The peak area ratios of test compound versus internal standard obtained was used to determine the fraction of compound remaining. Calculate the CL_{int} (μ l/min/mg protein) and recovery (%) by using the equations as follows: $CL_{int} = k / \text{microsomal protein concentration}$; $\text{recovery} = 100 \times \text{Peak area ratio of 60 min study sample} / \text{Peak area ratio of 0 min study sample}$.

4.2.4. Direct inhibition on 5CYPs in HLM

This assay utilized a 100 μ l incubation system containing human liver microsomes (0.2 mg/ml), substrate mixture (Midazolam 10 μ M, Testosterone 100 μ M, Dextromethophan 10 μ M, Diclofenac 20 μ M, Phenacetin 100 μ M, (S)-(+)-Mephenytoin 100 μ M), 10 μ M test compound, which were preincubated for 5 min at 37°C in 100 mM phosphate buffer (pH 7.4). The selective inhibitors of each P450 isoform (Ketoconazole 10 μ M for CYP3A4, Quinidine 10 μ M for CYP2D6, Sulfaphenazole 100 μ M for CYP2C9, Naphthoflavone 10 μ M for CYP1A2, Tranylcypromine

1000 μM for CYP2C19) were used as positive controls. The reaction of test compound or positive controls was initiated by adding NADPH (1 mM) and the negative control was initiated by adding 100 mM phosphate buffer (pH 7.4). After 20 min incubations at 37°C, the reactions were stopped by adding 300 μl acetonitrile containing tinidazole of 0.1 $\mu\text{g}/\text{ml}$ as internal standards. The samples were vortexed for 10 min, and then centrifuged at 6000 g for 10 min twice at 4°C and an aliquot of supernatant was sampled for LC-MS/MS analysis. The peak area ratios of the substrate metabolites versus internal standard obtained was used to determine the relative activity of the enzyme. Calculate the Inhibition by using the equation as follows: $\text{Inhibition} = 100 \times (1 - \text{Peak area ratio of positive control or test compound} / \text{Peak area ratio of negative control})$.

4.2.5. Time-dependent inhibition on 5CYPs in HLM

This assay utilized a 200 μl incubation system containing human liver microsomes (0.2 mg/ml), 10 μM test compound, which were preincubated for 0 min, 5 min, 10 min and 20 min at 37°C after adding NADPH (1 mM) or PBS. Then the system was incubated for 10 min at 37°C after adding 180 μl secondary incubation mixture containing NADPH (1 mM) and substrate mixture (Midazolam 5 μM , Testosterone 50 μM , Dextromethophan 5 μM , Diclofenac 10 μM , Phenacetin 50 μM , (S)-(+)-Mephentyoin 50 μM). The selective inhibitors of each P450 isoform (Troleandomycin 10 μM for CYP3A4, Paroxetine 10 μM for CYP2D6, Tienilic Acid 10 μM for CYP2C9, Furafylline 10 μM for CYP1A2, (S)-(+)-Fluoxetine 100 μM for CYP2C19) were used as positive controls. The reactions were stopped by adding 600 μl acetonitrile containing tinidazole of 0.1 $\mu\text{g}/\text{ml}$ as internal standards. The samples were vortexed for 10 min, and then centrifuged at 6000 g for 10 min twice at 4°C and an aliquot of supernatant was sampled for LC-MS/MS analysis.

The peak area ratios of the substrate metabolites versus internal standard obtained was used to determine the relative activity of the enzyme. The K_{obs} ($\times 10^{-4}/\text{min}$) was the slope of time-relative activity curve.

4.2.6. *In vitro* kinase panel assays

Inhibition of compound **14** on 18-kinase panel activities were determined by measuring the phosphorylation level of FAM labeled peptide substrate in Caliper mobility shift assay. Into a black 384-well plate was added 5 μL /well of 5X compound in reaction buffer. Next, 10 μL of kinase buffer (50 mM HEPES pH7.5, 0.0015% Brij-35, 10 mM MgCl_2 and 2 mM DTT, containing different concentrations of each kinase) was added to each well. After 5-10 min preincubation, the kinase reaction was initiated by the addition of 10 μL FAM labeled peptide and ATP in kinase buffer. After 30-60 minutes incubation at 28°C, the enzyme reaction was stopped by 25 μL of stop buffer containing 100 mM HEPES pH7.5, 0.015% Brij-35, 0.2% coating reagent#3 and 50 mM EDTA. Data of % conversion rate was collected on the Caliper EZ Reader.

4.2.7. *In vivo* pharmacokinetic study

Rat. Male Sprague-Dawley rats (180-220 g) were fasted overnight but with free access to water before use. Two rats were intravenously injected with test compound at a dose of 3 mg/kg. Three rats were orally administered with test compound at a dose of 6 mg/kg. Blood samples (about 0.2 mL at each time point) were collected at 0, 2, 5, 15, 30, 60, 90, 120, 240, 360, 480 and 1440 min in polypropylene tubes with heparin sodium.

Sample preparation. All blood samples were immediately centrifuged at 8000 rpm for 5 min

and the plasmas were frozen at -20°C until analysis. For analysis, the plasma samples were prepared by protein precipitation, to 50 μL rat plasma, 200 μL acetonitrile with IS was added. The mixture was vortex-mixed thoroughly for 10 min at 1500 rpm, and then centrifuged at 6000 g for 10 min. The supernatant was transferred to another clean 96 deep-well plate and centrifuged again at 6000 g for 10 min. An aliquot of 50 μL supernatant was sampled for UPLC-MS/MS analysis.

4.2.8. *In vivo antitumor activity studies*

Animals. Female/male BALB/c nude mice (5-6 weeks old) were housed and maintained under specific pathogen free conditions. Animal procedures were performed according to institutional ethical guidelines of animal care.

Subcutaneous xenograft models in athymic mice. The SNU-5 at a density of 6×10^6 tumor cells in 200 μL or NCI-H1993 at a density of 7×10^6 tumor cells in 140 μL were injected s.c. into the right flank of nude mice. Tumor-bearing animals were sorted into groups with similar mean tumor volumes prior to treatment (usually 100-200 mm^3 for SNU-5 and 150-250 mm^3 for NCI-H1993). The mice were randomly assigned into control and treatment groups ($n = 7$ (NCI-H1993 model) or $n = 6$ (SNU-5 model) per group). Control groups were given vehicle alone, and treatment groups received compound **14** as indicated doses via oral administration once daily for 2 weeks in SNU-5 model and oral administration once daily for 3 weeks in NCI-H1993 model, respectively. The sizes of the tumors were measured twice per week using a caliper, and the tumor volume was calculated in cubic millimeter using the formula: $V = (A \times B^2)/2$, where A and B was the long and short diameters of the tumor, respectively. Body weights were monitored throughout the study as a gross measure of toxicity/morbidity. Tumor growth inhibition (TGI), expressed in percent (%),

was calculated using the formula: $100\% \times (1 - ((\text{treated}^{\text{final day}} - \text{treated}^{\text{day 0}})/(\text{control}^{\text{final day}} - \text{control}^{\text{day 0}})))$. Percent tumor regression (PTR), expressed in percent (%), was calculated using the formula: $100\% \times (\text{treated}^{\text{day 0}} - \text{treated}^{\text{final day}})/\text{treated}^{\text{day 0}}$.

Data from in vivo efficacy evaluation are presented as the mean \pm SEM. and significance were determined by Student's *t*-test. Differences were considered statistically significant at * $p < 0.05$, ** $p < 0.01$.

4.2.9. Metabolites identification in monkey cytosol

This assay utilizes a 200 μ l incubation system containing monkey cytosol (1.15 mg/mL) to incubate with 100 μ M test compound at 37°C in 100 mM phosphate buffer (pH 7.4). Menadione, an inhibitor of AO enzyme with a concentration of 100 μ M, was added into the incubation system to investigate the metabolic extent of AO. After 30 min incubation, the reactions were stopped by adding 400 μ l acetonitrile containing tinidazole of 0.1 μ g/ml as internal standard. The samples were vortexed for 10 min, and then centrifuged at 6000 g for 10 min twice at 4°C and an aliquot of supernatant is sampled for LC-MS/MS analysis.

Metabolites **M1** was synthesized from 6-bromo-*N*²-(1-(7-fluoroquinolin-6-yl)ethyl)pyrazine-2,3-diamine by methods analogous to those described in our published work [23] and was further separated by SFC (AD-H column (19 \times 250 mm, 5 μ m), detection wavelength: 254 nm, 40% *i*-PrOH (0.1% DEA)) in 98% ee. Metabolites **M2** was synthesized from (*S*)-7-fluoro-6-(1-(6-(1-methyl-1*H*-pyrazol-4-yl)-1*H*-imidazo[4,5-*b*]pyrazin-1-yl)ethyl)quinoline (compound **1**) with 3-chloroperoxybenzoic acid (MCPBA).

4.3. Molecular docking

The crystal structure of c-Met kinase in complex with PF4217903 (PDB ID: 3ZXZ) obtained from the protein data bank (PDB) was used for molecular docking with Ligandfit docking tool in Discovery Studio (DS) 2016 package. The complex structure obtained was firstly prepared using Prepare Protein protocol in Discovery Studio. All the water molecules were removed except for HOH2067. The docking site was derived from the position of the PF4217903 cocrystallized in the binding site of 3ZXZ. And all the ligands were prepared using Prepare Ligands protocol and Minimize Ligands protocol in Discovery Studio subsequently. To validate the docking method, the PF4217903 was used to carry out the Ligandfit docking experiment. The docking results were evaluated through comparison of the best docked binding mode with the experimental one. The RMSD was used to compare differences between the atomic distances of the docked poses and the real cocrystallized pose to measure docking reliability. The RMSD of the heavy atom is only about 0.15 Å. It indicated that the Ligandfit docking method is fit for the c-Met-small molecular ligand system. The best pose was outputted on the basis of PLP1 and the protein-ligand interactions. Compound **14** used in the docking study is (*S*)-configuration.

Acknowledgements

We thank NeoTrident Co., Ltd. for excellent docking assistance.

Supplementary Material

Supplementary material (including synthetic procedures of the intermediates **b1-b7**, **c1-c7**, and **d1-d7**, separation conditions and biological data of two enantiomers of racemate **14**) can be found in a separate electronic file (.doc).

REFERENCES

- [1] D.P. Bottaro, J.S. Rubin, D.L. Faletto, A.M.L. Chan, T.E. Kmieciak, G.F. Vande Woude, S.A. Aaronson, Identification of the hepatocyte growth factor receptor as the c-met proto-oncogene product, *Science* 251 (1991) 802-804.
- [2] S. Benvenuti, P.M. Comoglio, The met receptor tyrosine kinase in invasion and metastasis, *J. Cell. Physiol.* 213 (2007) 316-325.
- [3] N. Shinomiya, G.F. Vande Woude, Suppression of Met expression: a possible cancer treatment, *Clin. Cancer Res.* 9 (2003) 5085-5090.
- [4] C. Birchmeier, W. Birchmeier, E. Gherardi, G.F. Vande Woude, Met, metastasis, motility and more, *Nat. Rev. Mol. Cell Biol.* 4 (2003) 915-925.
- [5] G. Maulik, A. Shrikhande, T. Kijima, P.C. Ma, P.T. Morrison, R. Salgia, Role of the hepatocyte growth factor receptor, c-MET, in oncogenesis and potential for therapeutic inhibition, *Cytokine Growth Factor Rev.* 13 (2002) 41-59.
- [6] K. Sawada, A.E. Radjabi, N. Shinomiya, E. Kistner, H. Kenny, A.R. Becker, M.A. Turkyilmaz, R. Salgia, S.D. Yamada, G.F. Vande Woude, M.S. Tretiakova, E. Lengyel, c-MET overexpression is a prognostic factor in ovarian cancer and an effective target for inhibition of peritoneal dissemination and invasion, *Cancer Res.* 67 (2007) 1670-1679.

- [7] H.L. Cheng, B. Trink, T.S. Tzai, H.S. Liu, S.H. Chan, C.L. Ho, D. Sidransky, N.H. Chow, Overexpression of c-MET as a prognostic indicator for transitional cell carcinoma of the urinary bladder: a comparison with p53 nuclear accumulation, *J. Clin. Oncol.* 20 (2002) 1544-1550.
- [8] E. Lengyel, D. Prechtel, J.H. Resau, K. Gauger, A. Welk, K. Lindemann, G. Alantic, T. Richter, B. Knudsen, G.F. Vande Woude, N. Harneck, c-MET overexpression in node-positive breast cancer identifies patients with poor clinical outcome independent of Her2/neu, *Int. J. Cancer* 113 (2005) 678-682.
- [9] L. Lo Muzio, A. Farina, C. Rubini, E. Coccia, M. Capogreco, G. Colella, R. Leonardi, G. Campisi, F. Carinci, Effect of c-MET expression on survival in head and neck squamous cell carcinoma, *Tumor Biol.* 27 (2006) 116-121.
- [10] U. Drebber, S.E. Baldus, B. Nolden, G. Grass, E. Bollschweiler, H.P. Dienes, A.H. Hölscher, S.P. Mönig, Overexpression of c-MET as a prognostic indicator for gastric carcinoma compared to p53 and p21 nuclear accumulation, *Oncol. Rep.* 19 (2008) 1477-1483.
- [11] J.A. Engelman, K. Zejnullahu, T. Mitsudomi, Y. Song, C. Hyland, J.O. Park, N. Lindeman, C.M. Gale, X. Zhao, J. Christensen, T. Kosaka, A.J. Holmes, A.M. Rogers, F. Cappuzzo, T. Mok, C. Lee, B.E. Johnson, L.C. Cantley, P.A. Janne, Met amplification leads to gefitinib resistance in lung cancer by activating ERBB3 signaling, *Science* 316 (2007) 1039-1043.
- [12] P.Y. Shi, Y.T. Oh, G.J. Zhang, W.L. Yao, P. Yue, Y.K. Li, R. Kanteti, J. Riehm, R. Salgia, T.K. Owonikoko, S.S. Ramalingam, M.W. Chen, S.Y. Sun, Met gene amplification and protein hyperactivation is a mechanism of resistance to both first and third generation EGFR inhibitors in lung cancer treatment, *Cancer Lett.* 380 (2016) 494-504.

- [13] J.J. Cui, M. Tran-Dube, H. Shen, M. Nambu, P.P. Kung, M. Pairish, L. Jia, J. Meng, L. Funk, I. Botrous, M. McTigue, N. Grodsky, K. Ryan, E. Padrique, G. Alton, S. Timofeevski, S. Yamazaki, Q. Li, H. Zou, J. Christensen, B. Mroczkowski, S. Bender, R.S. Kania, M.P. Edwards, Structure based drug design of Crizotinib (PF-02341066), a potent and selective dual inhibitor of mesenchymal-epithelial transition factor (c-MET) kinase and anaplastic lymphoma kinase (ALK), *J. Med. Chem.* 54 (2011) 6342-6363.
- [14] S. Roy, B.K. Narang, S.K. Rastogi, R.K. Rawal, A novel multiple tyrosine-kinase targeted agent to explore the future perspectives of anti-angiogenic therapy for the treatment of multiple solid tumors: Cabozantinib, *Anti-Cancer Agent Me.* 15 (2015) 37-47.
- [15] J.J. Cui, M. McTigue, M. Nambu, M. Tran-Dube, M. Pairish, H. Shen, L. Jia, H.M. Cheng, J. Hoffman, P. Le, M. Jalaie, G.H. Goetz, K. Ryan, N. Grodsky, Y.L. Deng, M. Parker, S. Timofeevski, B.W. Murray, S. Yamazaki, S. Aguirre, Q.H. Li, H. Zou, J. Christensen, Discovery of a novel class of exquisitely selective mesenchymal-epithelial transition factor (c-MET) protein kinase inhibitors and identification of the clinical candidate 2-(4-(1-(quinolin-6-ylmethyl)-1*H*-[1,2,3]triazolo[4,5-*b*]pyrazin-6-yl)-1*H*-pyrazol-1-yl)ethanol (PF-04217903) for the treatment of cancer, *J. Med. Chem.* 55 (2012) 8091-8109.
- [16] D. Dorsch, O. Schadt, F. Stieber, M. Meyring, U. Grädler, F. Bladt, M. Friese-Hamim, C. Knühl, U. Pehl, A. Blaukat, Identification and optimization of pyridazinones as potent and selective c-Met kinase inhibitors, *Bioorg. Med. Chem. Lett.* 25 (2015) 1597-1602.
- [17] H. Nishii, T. Chiba, K. Morikami, T.A. Fukami, H. Sakamoto, K. Ko, H. Koyano, Discovery of 6-benzyloxyquinolines as c-Met selective kinase inhibitors, *Bioorg. Med. Chem. Lett.* 20 (2010) 1405-1409.

- [18] L. Wang, J. Ai, Y.Y. Shen, H.T. Zhang, X. Peng, M. Huang, A. Zhang, J. Ding, M.Y. Geng, SOMCL-863, a novel, selective and orally bioavailable small-molecule c-Met inhibitor, exhibits antitumor activity both *in vitro* and *in vivo*, *Cancer Lett.* 351 (2014) 143-150.
- [19] C.H. Park, S.Y. Cho, J.D. Ha, H. Jung, H.R. Kim, C.O. Lee, I. Jang, C.H. Chae, H.K. Lee, S.U. Choi, Novel c-Met inhibitor suppresses the growth of c-Met-addicted gastric cancer cells, *BMC cancer* 16 (2016) 35.
- [20] X.D. Liu, Q. Wang, G.J. Yang, C. Marando, H.K. Koblisch, L.M. Hall, J.S. Fridman, E. Behshad, R. Wynn, Y. Li, J. Boer, S. Diamond, C.H. He, M.Z. Xu, J.C. Zhuo, W.Q. Yao, R.C. Newton, P.A. Scherle, A novel kinase inhibitor, INCB28060, blocks c-MET-dependent signaling, neoplastic activities, and cross-talk with EGFR and HER-3, *Clin. Cancer Res.* 17 (2011) 7127-7138.
- [21] H. Jia, G.X. Dai, J.Y. Weng, Z.L. Zhang, Q. Wang, F. Zhou, L.X. Jiao, Y.M. Cui, Y.X. Ren, S.M. Fan, J.H. Zhou, W.G. Qing, Y. Gu, J. Wang, Y. Sai, W.G. Su, Discovery of (S)-1-(1-(imidazo[1,2-*a*]pyridin-6-yl)ethyl)-6-(1-methyl-1*H*-pyrazol-4-yl)-1*H*-[1,2,3]triazolo[4,5-*b*]pyrazine (Volitinib) as a highly potent and selective mesenchymal-epithelial transition factor (c-Met) inhibitor in clinical development for treatment of cancer, *J. Med. Chem.* 57 (2014) 7577-7589.
- [22] P.E. Hughes, K. Rex, S. Caenepeel, Y.J. Yang, Y.H. Zhang, M.A. Broome, H.T. Kha, T.L. Burgess, B. Amore, P.J. Kaplan-Lefko, J. Moriguchi, J. Werner, M.A. Damore, D. Baker, D.M. Choquette, J. Harmange, R. Radinsky, R. Kendall, I. Dussault, A. Coxon, *In vitro* and *in vivo* activity of AMG 337, a potent and selective MET kinase inhibitor, in MET-dependent cancer models, *Mol. Cancer Ther.* 15 (2016) 1568-1579.

- [23] F. Zhao, J. Zhang, L.D. Zhang, Y. Hao, C. Shi, G.X. Xia, J.X. Yu, Y.J. Liu, Discovery and optimization of a series of imidazo[4,5-*b*]pyrazine derivatives as highly potent and exquisitely selective inhibitors of the mesenchymal-epithelial transition factor (c-Met) protein kinase, *Bioorg. Med. Chem.* 24 (2016) 4281-4290.
- [24] S. Diamond, J. Boer, T.P. Maduskuie, N. Falahatpisheh, Y. Li, S. Yeleswaram, Species-specific metabolism of SGX523 by aldehyde oxidase and the toxicological implications, *Drug Metab. Dispos.* 38 (2010) 1277-1285.
- [25] L.B. Ye, Y.X. Tian, Z.H. Li, H. Jin, Z.G. Zhu, S.H. Wan, J.Y. Zhang, P.J. Yu, J.J. Zhang, S.G. Wu, Design, synthesis and molecular docking studies of some novel spiro[indoline-3,4'-piperidine]-2-ones as potential c-Met inhibitors, *Eur. J. Med. Chem.* 50 (2012) 370-375.
- [26] B.K. Albrecht, J.C. Harmange, D. Bauer, L. Berry, C. Bode, A.A. Boezio, A. Chen, D. Choquette, I. Dussault, C. Fridrich, S. Hirai, D. Hoffman, J.F. Larrow, P. Kaplan-Lefko, J. Lin, J. Lohman, A.M. Long, J. Moriguchi, A. O'Connor, M.H. Potashman, M. Reese, K. Rex, A. Siegmund, K. Shah, R. Shimanovich, S.K. Springer, Y. Teffera, Y.J. Yang, Y.H. Zhang, S.F. Bellon, Discovery and optimization of triazolopyridazines as potent and selective inhibitors of the c-Met kinase, *J. Med. Chem.* 51 (2008) 2879-2882.
- [27] H.L. Yuan, J. Zhuang, S.H. Hu, H.F. Li, J.X. Xu, Y.N. Hu, X. Xiong, Y.D. Chen, T. Lu, Molecular modeling of exquisitely selective c-Met inhibitors through 3D-QSAR and molecular dynamics simulations, *J. Chem. Inf. Model.* 54 (2014) 2544-2554.

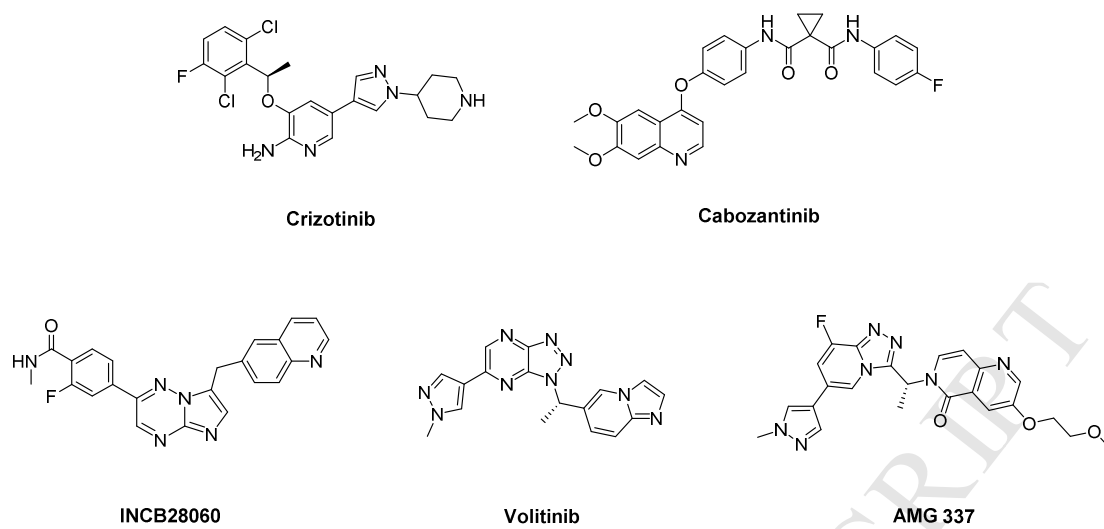


Fig. 1. Reference compounds.

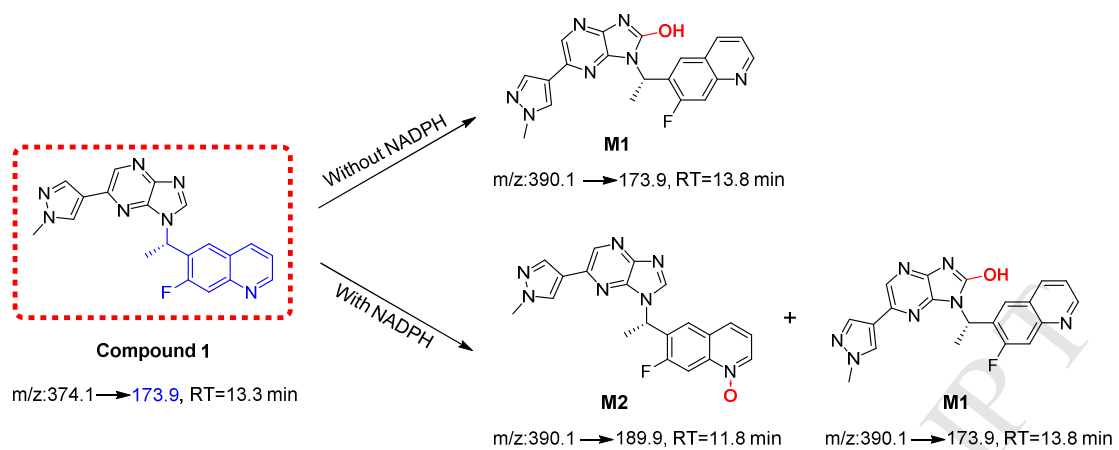


Fig. 2. Major metabolites of compound 1 in monkey liver microsomes incubated with or without NADPH.

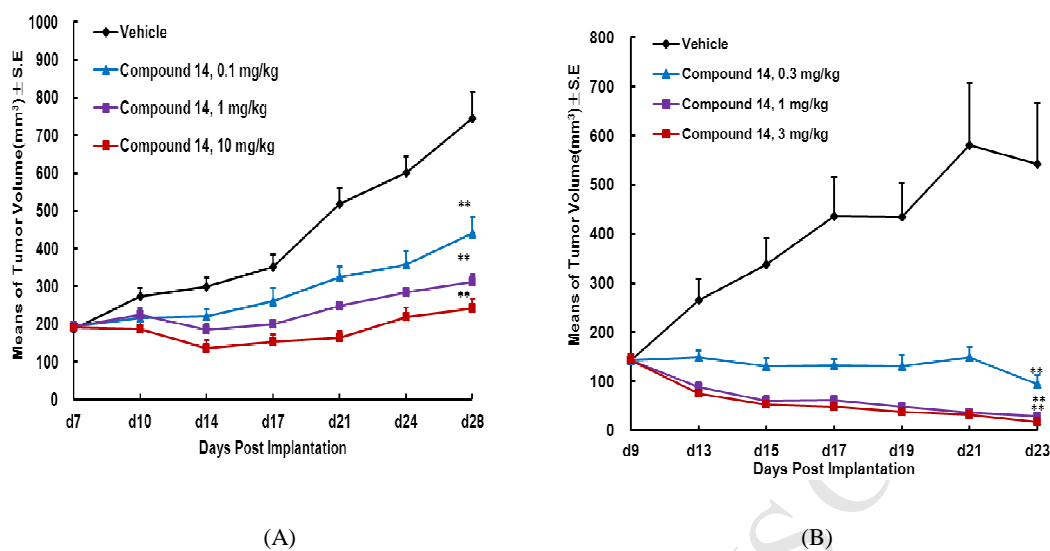


Fig. 3. (A) Growth inhibition of **14** in H1993 xenograft model in mice. Mice bearing H1993 tumors were orally administered **14** once daily at the indicated dose levels or vehicle alone for 3 weeks. (B) Growth inhibition of **14** in SNU-5 xenograft model in mice. Mice bearing SNU-5 tumors were orally administered **14** once daily at the indicated dose levels or vehicle alone for 2 weeks. Data represents the mean \pm SEM. for each group over the treatment period (n=6-7).

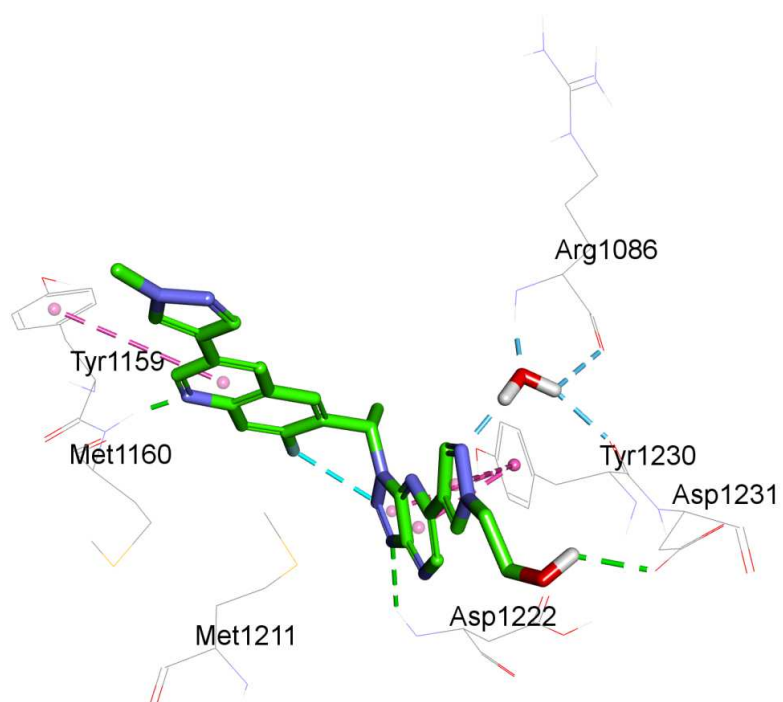
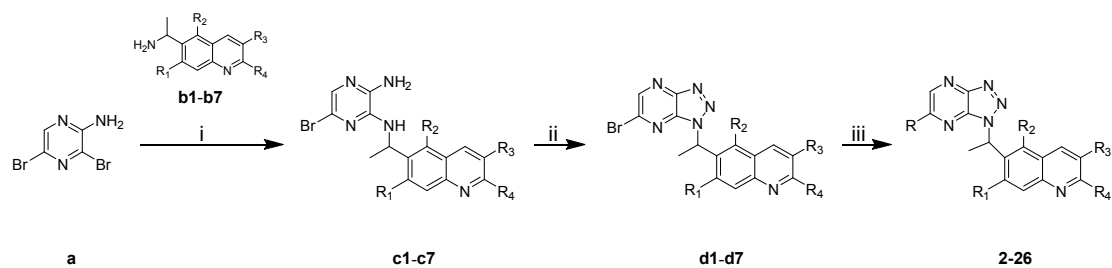
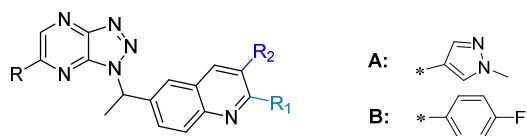


Fig. 4. Compound **14** was docked into the active site of c-Met.



$R_1, R_2 = \text{H or F}; R_3, R_4 = \text{N-methylpyrazol-4-yl or 4-fluorophenyl}$

Scheme 1. Synthetic procedures of title compounds **2-26**. Reagents and conditions: (i) DIPEA, NMP, 180°C, overnight; (ii) isopentyl nitrite, DMF, 80°C, 2h; (iii) corresponding boric acid or boric acid ester, Pd(dppf)₂Cl₂·DCM complex, K₂CO₃, 1,4-dioxane/H₂O, 110°C, 3h or overnight.

Table 1SAR of 2-substituted and 3-substituted quinoline derivatives **2-8**.

Compd.	R ₁	R ₂	R	IC ₅₀ ^a (nM)		
				Enzyme	H1993	SNU-5
1 [23]				1.5	24.7	11.8
2	-A	-H		>100	- ^b	- ^b
3	-A	-H		66.7	- ^b	- ^b
4	-A	-H		>100	- ^b	- ^b
5	-H	-A		0.5	- ^b	0.5
6	-H	-B		1.3	1.2	2.2
7	-H	-B		3.5	4.2	3.7
8	-H	-B		2.6	8.7	7.0
INCB28060				0.4	2.3	2.7

^aIC₅₀ are based on triple runs of experiments.^bThe – indicates not tested.

Table 2

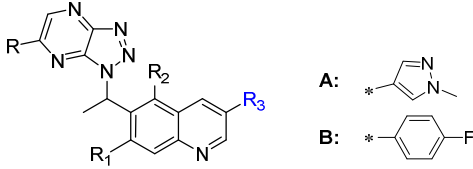
Metabolic stability data of compounds in liver microsomes among different species.

Compd.	CL _{int} (μl/min/mg protein) ^a / Parent drug recovery (%) ^b		
	HLM ^c	RLM ^d	MLM ^e
1	8 / 92	49 / 79	- ^f / 1
5	12 / 123	22 / 115	42 / 79
6	16 / 105	28 / 97	112 / 109
7	15 / 104	57 / 97	119 / 93
8	14 / 105	56 / 91	65 / 97

^aCL_{int} was determined with the cofactor NADPH; ^brecovery was determined without the cofactor NADPH; ^chuman liver microsomes; ^drat liver microsomes; ^emonkey liver microsomes; ^fThe-indicates the data was not obtained because of rapid metabolism of compound.

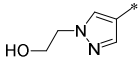
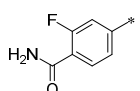
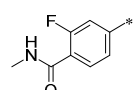
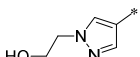
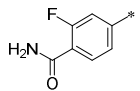
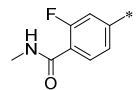
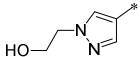
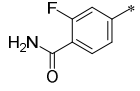
Table 3

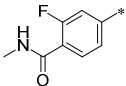
SAR about the 3-substituted quinoline derivatives.



A: 

B: 

Compd.	R ₁	R ₂	R ₃	R	IC ₅₀ ^a (nM)		
					Enzyme	H1993	SNU-5
9	-H	-H	-A		0.5	0.2	1.8
10	-H	-H	-A		0.7	0.9	0.7
11	-H	-H	-A		0.5	0.5	0.6
12	-H	-H	-A		0.3	0.9	1.2
13	-F	-H	-A		0.7	0.9	1.7
14	-F	-H	-A		0.6	1.1	2.0
15	-F	-H	-A		0.6	0.9	0.6
16	-F	-H	-A		1.0	1.1	0.6
17	-F	-H	-A		0.7	3.2	2.5
18	-F	-F	-A		0.4	0.8	1.3
19	-F	-F	-A		0.4	0.8	1.3
20	-F	-F	-A		0.3	0.4	0.4

21	-F	-F	-A		0.9	- ^b	0.9
22	-F	-F	-A		0.5	0.2	1.2
23	-F	-H	-B		1.5	4.1	2.0
24	-F	-H	-B		1.7	3.6	6.8
25	-F	-F	-B		3.8	2.6	2.2
26	-F	-F	-B		4.3	3.5	7.2
INCB28060					0.4	2.3	2.7

^aIC₅₀ are based on triple runs of experiments.

^bThe - indicates not tested.

Table 4Leadlikeness assessment *in vitro* of compounds **9-22**.

Compd.	CL _{int} (µl/min/mg protein) / Parent drug recovery (%)			DI ^a	TDI ^b
	HLM	MLM	RLM		
9	0 / 105	16 / 108	6 / 104	2C9,2C19	NI ^c
10	3 / 120	30 / 98	10 / 128	NI ^c	3A4,2D6,2C9,1A2
11	1 / 115	16 / 97	5 / 114	3A4	NI ^c
12	22 / 104	78 / 90	61 / 94	3A4	NI ^c
13	5 / 101	11 / 65	34 / 103	NI ^c	3A4
14	5 / 95	50 / 107	5 / 101	NI ^c	NI ^c
15	2 / 120	6 / 103	1 / 115	NI ^c	NI ^c
16	5 / 116	24 / 69	12 / 111	NI ^c	NI ^c
17	4 / 113	49 / 103	55 / 106	3A4,2C9,2C19	NI ^c
18	17 / 91	86 / 75	22 / 94	2C9,2C19	3A4
19	8 / 98	43 / 102	20 / 97	2C9, 2C19	NI ^c
20	11 / 97	50 / 99	12 / 94	NI ^c	3A4
21	5 / 92	187 / 95	48 / 95	2C9, 2C19	NI ^c
22	9 / 101	106 / 99	26 / 98	3A4,2D6,2C9,2C19	NI ^c

^adirect inhibition on 5CYPs in HLM, referred to reversible inhibition, is assessed without a preincubation step.

^btime-dependent inhibition on 5CYPs in HLM, referred to irreversible inhibition, is assessed with a preincubation

step. ^cThe NI indicates inhibition ratio < 50%.

Table 5

In vivo pharmacokinetic profiles^a of compounds **14** and **15**.

Compd.	CL _{plasma} ^b (L/h/kg)	V _{ss} ^b (L/kg)	T _{1/2} ^b (h)	C _{max} ^c (ng/ml)	AUC _{0-24h} ^c (ng·h/ml)	F ^c (%)
14	0.58	2.1	3.7	134.6	1254	12.1
15	0.56	2.0	3.2	98.9	879	8.2

^aExperiments were carried out with male Sprague-Dawley rats (n=2-3). Dose: iv, 1mg/kg; po, 6 mg/kg.

^bParameters obtained after iv dosing. ^cParameters obtained after po dosing.

Table 6Kinase-selectivity profile^a of compound **14**.

kinase	IC ₅₀ (nM)	kinase	IC ₅₀ (nM)
AxI	1075	EGFR	>30000
RON	731	EGFR[T790]	>30000
ALK	>30000	ErbB4	>30000
Fit-1	>30000	c-Src	17056
VEGFR2	18364	ABL	>30000
c-Kit	5396	EPH-A2	>30000
PDGFRa	2357	EPH-B2	>30000
PDGFRb	>30000	IGF1R	>30000
RET	>30000	FGFR1	>30000

^aCompound **14** against 18 kinases *in vitro* were assayed with ATP concentration at Km.

Identification of

3-substituted-6-(1-(1*H*-[1,2,3]triazolo[4,5-*b*]pyrazin-1-yl)ethyl)quinoline derivatives as highly potent and selective mesenchymal-epithelial transition factor (c-Met) inhibitors via metabolite profiling-based structural optimization

Fei Zhao, Le-Duo Zhang, Yu Hao, Na Chen, Rui Bai, Yu-Ji Wang, Chun-Chun Zhang, Gong-Sheng Li, Li-Jun Hao, Chen Shi, Jing Zhang, Yu Mao, Yi Fan, Guang-Xin Xia, Jian-Xin Yu*, Yan-Jun Liu*

Central Research Institute, Shanghai Pharmaceuticals Holding Co., Ltd., Building 5, No. 898 Halei Road, Shanghai 201203, P. R. China

Highlights

- A novel series of 3-substituted-6-(1-(1*H*-[1,2,3]triazolo[4,5-*b*]pyrazin-1-yl)ethyl)quinoline derivatives as highly potent c-Met inhibitors was rationally designed based on metabolite profiling of lead compound **1**.
- Designed compounds demonstrated remarkable inhibitory activities in cellular assays and were stable in liver microsomes among different species.
- Compound **14** exhibited significant antitumor efficacy in both H1993 and SNU-5 xenograft models.
- Docking analysis was performed to elucidate the binding mode.

* Corresponding authors. Tel.: +86 21 61871700; Fax: +86 21 50128885.
E-mail addresses: yujx@sphchina.com (J.-X. Yu), liuyj@sphchina.com (Y.-J. Liu).